Radio resource management for V2V multihop communication considering adjacent channel interference

Downloaded from: https://research.chalmers.se, 2024-04-17 10:04 UTC

Citation for the original published paper (version of record):
Unnichiriyath Siddique, A., Ström, E., Brännström, F. (2021). Radio resource management for V2V multihop communication considering adjacent channel interference. IEEE Transactions on Intelligent Transportation Systems, 22(11): 7084-7101. http://dx.doi.org/10.1109/TITS.2020.3001366

N.B. When citing this work, cite the original published paper.

© 2021 IEEE. Personal use of this material is permitted. Permission from IEEE must be obtained for all other uses, in any current or future media, including reprinting/republishing this material for advertising or promotional purposes, or reuse of any copyrighted component of this work in other works.

This document was downloaded from http://research.chalmers.se, where it is available in accordance with the IEEE PSPB Operations Manual, amended 19 Nov. 2010, Sec, 8.1.9. (http://www.ieee.org/documents/opsmanual.pdf).

(article starts on next page)

Radio Resource Management for V2V Multihop Communication Considering Adjacent Channel Interference

Anver Hisham, Erik G. Ström, *Senior Member, IEEE*, and Fredrik Brännström, *Member, IEEE*

***Abstract*— This paper investigates schemes for multihop scheduling and power control for vehicle-to-vehicle (V2V) multicast communication, taking into account the effects of both co-channel interference and adjacent channel interference, such that requirements on latency or age of information (AoI) are satisfied. Optimal performance can be achieved by formulating and solving mixed Boolean linear programming (MBLP) optimization problems for various performance metrics, including network throughput and connectivity. Fairness among network nodes (vehicles) is addressed by considering formulations that maximizes the worst-case network node performance. Solving the optimization problem comes at the cost of significant computational complexity for large networks and requires that (slow) channel state information is gathered at a central point. To address these issues, a clustering method is proposed to partition the optimization problem into a set of smaller problems, which reduces the overall computational complexity, and a decentralized algorithm that does not need channel state information is provided.**

I. Introduction

A. Motivation

V2V communications have drawn great attention due to its ability to improve traffic safety and efficiency. V2V communication can reduce accidents by broadcasting up-to-date local and emergency information. To this end, both periodic and event-driven messages are conveyed.

Periodic messages are broadcasted by all vehicles to inform neighbors about their current state, i.e., position, speed, heading, acceleration, etc, while event-driven messages are sent when an emergency situation has occurred. To this end, European Telecommunications Standards Institute (ETSI) is standardizing both cooperative awareness messages (CAMs) for periodic messages, and decentralized environmental notification messages (DENMs) for aperiodic messages. CAMs are sent with frequency 2–100 Hz with proposed latency requirements of 3–100 ms, depending upon the application [1]. DENMs are used to alert vehicles of a detected event, and the transmission can be repeated and persisted as long as the event is present [2]. However, both periodic and aperiodic messages in V2V are broadcast and localized in its nature, in order to facilitate cooperation between vehicles in close proximity.

In this work, we focus on safety-critical V2V applications and these applications have stringent requirements on latency and reliability. Latency is typically defined as the end-to-end delay a message experiences and reliability is the probability that the latency does not exceed the latency requirement. In a V2V setting, the latency metric is mainly applicable to DENM messages, as consecutive DENM messages are generally not interrelated. On the other hand, CAM messages carry periodic state updates and consecutive messages are clearly interrelated. For such data traffic, the age of information (AoI) metric is more applicable. The AoI, at a particular receiver, is the age of the latest received message. The AoI is therefore a non-negative random process, and performance can be expressed in terms of its statistics, i.e., the peak or the time-average of AoI [3]. AoI has been studied in V2V context in detail in [4].

The latency and AoI of a communication link is strongly affected by the packet error probability. The packet error probability is determined by signal to interference and noise power ratio (SINR), which in turn depends upon the received interference power. There are two main types of interference: co-channel interference (CCI) and adjacent channel interference (ACI). CCI is the cross-talk between transmitters scheduled in the same time-frequency slot, while ACI is the interference due to the leakage of transmit power outside the intended frequency slot. Therefore, ACI affects transmissions scheduled in neighbouring frequency slots within a timeslot.

Typically, ACI is negligible compared to CCI when the ACI interferers are not very much closer to the receiver compared to the desired transmitter. This is usually the case in cellular downlink/uplink communication, therefore, ACI is not a determining factor for SINR in this case. However, in V2V communication, distances from receiver to transmitters and interferers can be highly varying. Furthermore, the penetration loss by blocking vehicles increases with respect to the carrier frequency [5], and can be significant for V2V communication at 5.9 GHz [6]–[9]. This implies that the received power from a far-away transmitter is quite low compared to the received power from a near-by transmitter, especially when there are many blocking vehicles. Consequently, if the desired

Anver Hisham is a research engineer in Combitech, Gothenburg, Sweden. Erik G. Ström, and Fredrik Brännström are with the Communication Systems Group, Department of Electrical Engineering, Chalmers University of Technology, Gothenburg, Sweden. E-mail: anver.hisham@combitech.se, {erik.strom, fredrik.brannstrom}@chalmers.se.

The research was funded and performed in the framework of the H2020 project 5GCAR co-funded by the EU. The authors would like to acknowledge the contributions of their colleagues. The views expressed in this paper do not necessarily represent the project.

transmitter is far-away compared to the interferer (resulting in a so-called near-far situation), the ACI from the interferer can be a significant problem and determining factor for SINR [10], [11].

Even though, there exists many methods to suppress ACI, ACI can never be completely eliminated. This is because, ACI is mainly caused by the nonlinearities of the power amplifier (PA) in the transmitter and the clipping effect of the PA can never be avoided, even with advanced linearization techniques [12]–[15]. In this paper, we develop radio resource management (RRM) schemes (i.e., scheduling and power control) for direct V2V communication considering the effects of both ACI and CCI.

Hence, the V2V connectivity even over short distances can be prevented by the penetration loss due to blocking vehicles or buildings. To enable connectivity in these cases requires multihop (relaying) communication—either through 1) fixed infrastructure, e.g., via an uplink/core-network/downlink, or 2) a number of V2V direct links. There are pros and cons with each arrangement, however, the latter case is the only option when vehicles are outside coverage of the fixed infrastructure. Even when inside coverage, if the source and destination are relatively close to each other, it might be more resource efficient to multihop via vehicles rather than via the fixed infrastructure [16]. Moreover, lower range of V2V communication allows spectrum re-usage within a small area, while the large range of fixed infrastructure limits its possibilities.

B. Main Goal

The main goal of this paper is to formulate multihop scheduling and power control schemes such that requirements on latency or AoI for V2V multicast communication are satisfied, while taking both CCI and ACI into account.

C. State of the Art

There exists many studies on scheduling for V2V communication that consider reliability and latency requirements [17]–[19]. V2V scheduling algorithms for broadcast services are studied in [20], [21]. Out-of-cellular coverage scenario for V2V is studied theoretically in [22], and simulation-based in [23]. Infrastructure-based and distributed autonomous based scheduling are studied in [24] and [21] respectively. Location-based scheduling for a highway platooning scenario is investigated in [25], [26]. A scheduling strategy based on inter-VUE distances and mobility is proposed in [27] to improve the connectivity and reduce the access delay. In [28], a joint scheduling and power control algorithm is proposed for V2V networks with the objective to satisfy certain delay aware quality of service (QoS) requirements, under the assumption of instantaneous channel state information (CSI) knowledge. The authors prove that the optimal power allocation scheme in theory converges to the classical water-filling policy with the considered objective. Similar line of studies are done in [29] in the absence of CSI. A study on maximum achievable V2V datarates has been done in [30], where a network coding technique is proposed to cancel the interference. In [30], the authors consider road side unit (RSU) for the information exchange and propose a network coding technique to cancel the interference. The same paper studies the maximum achievable V2V datarates. In [31] and [32], the authors conclude that the IEEE 802.11p standard may not be sufficient to satisfy stringent V2V requirements. Instead, the authors suggests a novel medium access control (MAC) protocol and transport layer for IEEE 802.11p in order to satisfy real-time V2V requirements.

As already mentioned, ACI is not a significant problem in cellular communication, therefore, most of the existing literature focuses solely on mitigating CCI alone without considering ACI [24], [29], [33]. Still, the impact of ACI for cellular uplink communication and device-to-device (D2D) communication has been analyzed in [34] and [35] respectively. The impact of ACI on 802.11b/g/n/ac has also been broadly studied [36]–[38]. All these studies generally conclude that ACI causes outage and performance degradation. Additionally, for V2V communication with carrier-sense multiple access (CSMA) MAC layer, ACI can cause a potential transmitter to falsely assume that the channel is busy resulting in deferring transmissions [39], [40].

Multihop communication in V2V has also gained much attention recently, e.g., see [41]–[43], and references therein. In [41], an optimization problem is formulated to maximize the throughput and minimize latency using multihop routing. A theoretical analysis on the packet error probability bounds for multihop communication has been done in [44], and the authors conclude that 1-hop communication is favorable when vehicle density is low. In [45], authors approach multihop scheduling from a graph theoretic point of view and propose novel algorithms. Minimizing average AoI in vehicular networks has also captured attention and widely studied recently in [4], [46]–[48].

However, none of the above studies on scheduling or power control considers the effects of ACI. Furthermore, there is no study which combines multihop scheduling and AoI. Our previous studies [10], [11] try to find efficient scheduling and power control algorithms while taking into account the effects of ACI. In this paper, we generalize our previous works in mainly four directions: 1) allowing for multihop communication, 2) considering AoI as a performance metric, 3) introducing clustering to ensure scalability, 4) proposing a distributed scheduling algorithm.

D. Contributions

We make the following contributions in this paper:

1) The joint scheduling and power control problem to maximize the average/worst-case throughput and connectivity of a V2V network are formulated as MBLP problems.
2) Similar problem formulations are done to maximize connectivity with certain requirements on latency and AoI.
3) Due to the high computational complexity in finding optimal scheduling and power values for large networks,

TABLE I: Mathematical Notations

Symbol	Definition
x_i	i^{th} element of vector x
$X_{i,j}$	$(i,j)^{\text{th}}$ element of matrix $\mathbf{X}$
$\lvert\mathbf{X}\rvert$	Number of elements in matrix $\mathbf{X}$
$\lvert\mathcal{X}\rvert$	Cardinality of set $\mathcal{X}$
$\emptyset$	Empty set
$a \bmod b$	remainder of a when divided by b
$\lceil\cdot\rceil$	Ceil operation
$\lfloor\cdot\rfloor$	Floor operation
$\vee$	Boolean OR operation
$\wedge$	Boolean AND operation
$\neg$	Boolean NOT operation

we propose a clustering based algorithm which reduces computational complexity to ensure scalability.

4) A low-complexity, cluster-based distributed scheduling algorithm is proposed, in which a vehicular user equipment (VUE) is required to know only its position index, network size, and cluster size.
5) In all the problem formulations and proposed algorithms in this paper, we allow multihop communication and optimize considering the effects of both CCI and ACI.

E. Notation and Outline

We use the notations shown in Table I. Lowercase and uppercase letters, e.g., x and X, represent scalars. Lowercase boldface letter, e.g., $\mathbf{x}$, represent a vector, uppercase boldface letter, e.g., $\mathbf{X}$, represent a matrix, and calligraphic letters, e.g., $\mathcal{X}$, represent a set.

The logical flow towards the main goal of this paper (stated in Section I-B) is as follows: We start by providing the system model and basic assumptions in Section II. A general framework for scheduling and power control is then provided in Section III in terms of a MBLP, and we show in III-C that it can be formulated to maximize connectivity while satisfying latency or AoI requirement for each link. Moreover, even if this is not the main goal, we show how to modify the optimization problem to maximize network throughput or connectivity. Although optimal performance is achieved by solving the corresponding optimization problem, this comes at the cost of significant computational complexity for large networks and requires slow channel state information at a central point. To address these problems, we therefore partition the optimization problem into a set of smaller problems in Section IV, which reduces the overall computational complexity. We provide a decentralized algorithm, which does not require channel state information, in Section V. The resulting trade-offs between complexity is shown in Section VI and performance for the algorithms are illustrated by simulations in Section VII. Finally, conclusions are drawn in Section VIII.

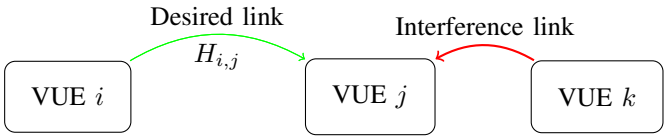

Fig. 1: System model

II. System Model

We consider a network of N VUEs in the set

$$\mathcal{N} \triangleq \{0, 1, \cdots, N-1\} \tag{1}$$

In general, we denote the transmitting, receiving, and interfering VUEs with i, j, and k, respectively, as illustrated in Fig. 1. The link (i,j) indicates the link from VUE i to VUE j. We consider multicast communication, which includes unicast and broadcast as special cases. We define $\mathcal{R}_i \subset \mathcal{N}$ as the set of *intended receivers* to VUE i. That is, VUE i wish to transmit its messages to the VUEs in $\mathcal{R}_i$. Clearly, $|\mathcal{R}_i| = 1$ and $\mathcal{R}_i = \mathcal{N} \setminus \{i\}$ implies that VUE i use unicast communication and broadcast communication, respectively.

In total, M messages are generated in the network during the scheduling interval. The available time-frequency resources are divided into T timeslots and F frequency slots. A time-frequency slot is called a resource block (RB) and is denoted as (f,t), where

$$f \in \mathcal{F} \triangleq \{0, 1, \ldots, F-1\}, \tag{2}$$

$$t \in \mathcal{S} \triangleq \{0, 1, \ldots, T-1\}. \tag{3}$$

For simplicity, we assume that the message

$$m \in \mathcal{M} \triangleq \{0, 1, \ldots, M-1\} \tag{4}$$

can be transmitted in a single RB. If a message is too large to fit into an RB, then it has to be scheduled in multiple RBs as explained in Appendix B-A. The maximum transmit power of a VUE is $P^{\max}$.

The parameter $H_{i,j}$ is the average channel power gain from VUE i to VUE j. Hence, $H_{i,j}$ takes into account pathloss, penetration loss and large-scale fading between VUE i and VUE j. We assume that $H_{i,j}$ is fixed during the scheduling interval (i.e., for T timeslot durations) and known to the scheduling and power control algorithms. For practical V2V channels, this implies that the scheduling interval is on the order of 100 ms. The small-scale fading (fast fading) distribution is assumed to be known. However, the fast fading *realization* is not assumed to be known, as this would require a potentially very large CSI measurement and feedback overhead.

Suppose VUE i is transmitting in RB (f,t) and VUE k in RB (f',t'). If $t' \neq t$, then there will be no interference, since timeslots are assumed to be orthogonal. If $t' = t$, then there will CCI if $f' = f$ and ACI if $f' \neq f$. In this paper, we consider the effects of both CCI and ACI. It can be shown that the transmitted message will be received with an error probability less than ϵ if the SINR (as defined in (14) below) is equal or larger than a certain threshold γ^{T}. The

TABLE II: Key Mathematical Symbols

Symbol	Definition
Parameters	
N	Number of VUEs
F	Number of frequency slots
T	Number of timeslots
M	Total number of messages to transmit
$H_{i,j}$	Average channel power gain from VUE i to VUE j
λ_r	ACI from any frequency slot f to frequency slot $f \pm r$
σ^2	Noise power in an RB
γ^{T}	SINR threshold to declare a link is successful
$P^{\max}$	Maximum transmit power of a VUE
$\mathcal{M}_i$	Set of messages generated by VUE i
t_m^{gen}	Generation time of message m
$\Omega_{i,m,t}$	Indicate if VUE i can transmit the message m at the earliest timeslot t
Variables	
$\mathcal{R}_i$	Set of receivers for Tx-VUE i
$P_{i,f,t}$	Transmit power of VUE i in an RB in timeslot t
$S_{i,j,f,t}$	Received power by VUE j from VUE i in RB (f,t)
$R_{j,f,t}$	Total received power by VUE j in RB (f,t)
$X_{i,m,f,t}$	Indicate if VUE i is scheduled to transmit message m in RB (f,t)
$Y_{i,j,f,t}$	Indicate if link (i,j) is successful in RB (f,t)
$W_{j,m,t}$	Indicate if VUE j receives message m during timeslot t
$Z_{i,j}$	Indicate if link (i,j) is connected or not
$A_{i,j,t}$	AoI of the link (i,j) during timeslot t
$\tau_{j,m}$	Latency of message m upon reception by VUE j
C	Number of clusters
G	Number of groups
N^{Tx}	Number Tx-VUEs in a group
$\mathcal{T}^{(c,g)}$	Set of Tx-VUEs in group (c,g)
$\mathcal{R}^{(c,g)}$	Set of Rx-VUEs in group (c,g)
$\mathcal{S}_g$	Set of timeslots for group g

threshold can computed for any given ϵ and small-scale fading distribution [49, Lemma 1].

In general, scheduling and power control is done by a controller. As mentioned above, we assume that large-scale channel parameters (i.e., pathloss, shadowing, and penetration loss) are slowly varying compared to the scheduling interval T and that the controller has access to this slowly varying CSI for all relevant VUE pairs. A base station (BS), intelligent transport system stations (ITS-S), or a specially assigned VUE can act as the controller. In this paper, we will consider the case when the network has a single controller, multiple controllers, and when each VUE acts as its own controller.

III. Joint Scheduling and Power Control

In this section, joint scheduling and power control problem to maximize various objectives are formulated as an MBLP problem. Note that, all Boolean operations (like AND, OR, ... etc) can be translated into linear operations with Boolean variables as explained in Appendix A. Key mathematical symbols are listed in Table II.

A. Variables and Constraints Formulations

In this section, we will define a number of variables and constraints that are indexed by i, j, m, f, and t. If not explicitly stated otherwise, the definitions are valid for $i \in \mathcal{N}$, $j \in \mathcal{N}$, $m \in \mathcal{M}$, $f \in \mathcal{F}$, and $t \in \mathcal{S}$.

1) Message generation time: We assume that a VUE generates a message m at time $t_m^{\mathrm{gen}} \in \mathbb{R}$, and that it is available for transmission on or after time $t_m^{\mathrm{gen}} + t^{\mathrm{d}}$, where $t^{\mathrm{d}} \in \mathbb{R}^+$ is the minimum time delay between message generation and transmission. Both t_m^{gen} and t^{d} are assumed to be measured in terms of number of timeslot durations, e.g., the packet is available for transmission t^{d} timeslots after the generation of the packet.

We define the parameter $\Omega_{i,m,t} \in \{0,1\}$ to indicate if VUE i generates the message m and it is available for transmission at the earliest timeslot t, i.e.,

$$\Omega_{i,m,t} \triangleq \begin{cases} 1, & \text{if VUE } i \text{ generates message } m \\ & \text{during timeslot } \lfloor t - t^{\mathrm{d}} \rfloor \\ 0, & \text{otherwise.} \end{cases} \tag{5}$$

That is, if $\Omega_{i,m,t} = 1$, then the message m is available for transmission on or after the timeslot t. We assume that the message arrivals are deterministic, hence, $\Omega_{i,m,t}$ is known in the optimization problems. We denote the set of messages generated by VUE i as

$$\mathcal{M}_i \triangleq \{m \in \mathcal{M} : \Omega_{i,m,t} = 1, t \in \mathcal{S}\}. \tag{6}$$

2) Scheduling constraints: The elements of the scheduling matrix $\mathbf{X} \in \{0,1\}^{N \times N \times F \times T}$ are the variables

$$X_{i,m,f,t} \triangleq \begin{cases} 1, & \text{if VUE } i \text{ is scheduled to transmit} \\ & \text{message } m \text{ in RB } (f,t) \\ 0, & \text{otherwise.} \end{cases} \tag{7}$$

A VUE can transmit at most one message in an RB. Hence, since

$$\tilde{X}_{i,f,t} = \sum_{m \in \mathcal{M}} X_{i,m,f,t} \tag{8}$$

indicates if VUE i is transmitting in RB (f,t), the constraint is

$$\tilde{X}_{i,f,t} \leq 1. \tag{9}$$

3) Transmit power constraints: The transmit power matrix is denoted $\mathbf{P} \in [0, P^{\max}]^{N \times F \times T}$, where $P_{i,f,t}$ is the transmit power of VUE i in RB (f,t). The variable $P_{i,f,t}$ is constrained by the maximum transmit power $P^{\max}$ of a VUE:

$$\sum_{f \in \mathcal{F}} P_{i,f,t} \leq P^{\max} \tag{10}$$

Furthermore, $P_{i,f,t}$ is also constrained by scheduling as

$$0 \leq P_{i,f,t} \leq P^{\max} \tilde{X}_{i,f,t}. \tag{11}$$

4) SINR constraints: Suppose VUE i transmits a message to VUE j in RB (f,t). The desired signal power at VUE j is

$$S_{i,j,f,t} = P_{i,f,t} H_{i,j}, \tag{12}$$

and the total received signal power (desired plus interference) is

$$R_{j,f,t} = \sum_{f' \in \mathcal{F}} \sum_{k \in \mathcal{N}} P_{k,f',t} H_{k,j} \lambda_{|f'-f|}, \tag{13}$$

where λ_r is the adjacent channel interference ratio (ACI) from a frequency slot f to frequency slot $f \pm r$ [50, section 17.9]. Therefore, $\lambda_{|f'-f|}$ is the inverse-ACI from frequency slot f' to f, see Fig. 2. In other words, $\lambda_{|f'-f|}$ is the ratio of the received interference power in frequency slot f to the received interference power in frequency slot f' when the interfering VUE is transmitting in frequency slot f'. Note that when $f' = f$, then the interference is CCI instead of ACI. Therefore, to accommodate CCI and to make (13) correct, we set $\lambda_0 = 1$.

Following (12) and (13), we can compute the SINR for the link (i,j) in RB (f,t) as

$$\gamma_{i,j,f,t} = \frac{S_{i,j,f,t}}{\sigma^2 + (R_{j,f,t} - S_{i,j,f,t})}, \tag{14}$$

where σ^2 is the noise power in an RB.

The link (i,j) is said to be *successful* in RB (f,t) if the $\gamma_{i,j,f,t} \geq \gamma^{\mathrm{T}}$, which implies that the error probability is at most $\epsilon(\gamma^{\mathrm{T}})$ (see Appendix B-B for further details). By substituting (14) into $\gamma_{i,j,f,t} \geq \gamma^{\mathrm{T}}$ and solving for $S_{i,j,f,t}$ yields the constraint

$$S_{i,j,f,t} \geq \bar{\gamma}^{\mathrm{T}} (\sigma^2 + R_{j,f,t}), \tag{15}$$

where

$$\bar{\gamma}^{\mathrm{T}} \triangleq \frac{\gamma^{\mathrm{T}}}{1+\gamma^{\mathrm{T}}}. \tag{16}$$

However, it might not be feasible to satisfy (15) for all links (i,j) in all RBs (f,t). To select which combinations of i, j, f, and t to enforce the SINR constraint, we introduce the matrix $\mathbf{Y} \in \{0,1\}^{N \times N \times F \times T}$, where

$$Y_{i,j,f,t} \triangleq \begin{cases} 1, & \text{if (15) is enforced} \\ 0, & \text{otherwise} \end{cases} \tag{17}$$

We can combine (15) and (17) into a single constraint,

$$S_{i,j,f,t} \geq \bar{\gamma}^{\mathrm{T}} (\sigma^2 + R_{j,f,t}) - \zeta (1 - Y_{i,j,f,t}) \tag{18}$$

where ζ is a sufficiently large number to make (18) hold whenever $Y_{i,j,f,t} = 0$, regardless of the schedule and power allocation. It is not hard to show that $\zeta = \bar{\gamma}^{\mathrm{T}} (\sigma^2 + N P^{\max})$ is sufficient. Observe that if $Y_{i,j,f,t} = 1$, then the link (i,j) is successful in RB (f,t) if (18) is satisfied.

To make it explicit which optimization variables that affect the SINR constraint, we substitute (12) and (13) into (18), which yields

$$P_{i,f,t} H_{i,j} \geq \bar{\gamma}^{\mathrm{T}} (\sigma^2 + \sum_{f' \in \mathcal{F}} \sum_{k \in \mathcal{N}} P_{k,f',t} H_{k,j} \lambda_{|f'-f|}) - \zeta (1 - Y_{i,j,f,t}). \tag{19}$$

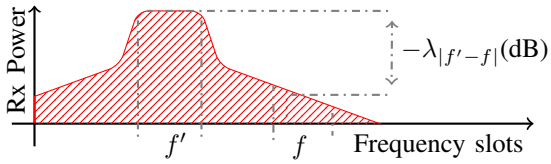

Fig. 2: Received power (dBm) when an interferer is transmitting in frequency slot f'

5) Message reception constraints: We define the matrix $\mathbf{W} \in \{0,1\}^{N \times M \times T}$ with elements

$$W_{j,m,t} \triangleq \begin{cases} 1, & \text{if message } m \text{ is scheduled to VUE } j \text{ with SINR} \geq \gamma^{\mathrm{T}} \text{ for the first time in timeslot } t, \\ 0, & \text{otherwise} \end{cases} \tag{20}$$

We can compute $W_{j,m,t}$ as

$$W_{j,m,t} = \Big(\bigvee_{i \in \mathcal{N}} \bigvee_{f \in \mathcal{F}} X_{i,m,f,t} \wedge Y_{i,j,f,t} \Big) \wedge \Big(\neg \bigvee_{t'=0}^{t-1} W_{j,m,t'} \Big) \tag{21}$$

where the *AND* operation with $(\neg \bigvee_{t'=0}^{t-1} W_{j,m,t'})$ is to ensure that the message m has not already been received in any of the previous timeslots $t' < t$.

If $W_{j,m,t} = 1$, then VUE j can relay (i.e., transmit) the message m during or after timeslot $\lceil t + t^{\mathrm{p}} \rceil$, where $t^{\mathrm{p}} \in \mathbb{R}^+$ is the processing delay (measured in timeslots) for a VUE to relay a message. It should be noted that VUE i can transmit message m during timeslot t if and only if (a) VUE i generates the message on or before timeslot $\lfloor t - t^{\mathrm{d}} \rfloor$ or (b) VUE i receives the message from some other VUEs on or before timeslot $\lceil t - t^{\mathrm{p}} \rceil$. In other words, the Boolean variable $X_{i,m,f,t}$ is constrained as[1],

$$X_{i,m,f,t} \leq \Big(\bigvee_{t'=0}^{t} \Omega_{i,m,t'} \Big) \vee \Big(\bigvee_{t'=0}^{\lceil t - t^{\mathrm{p}} \rceil} W_{i,m,t'} \Big). \tag{22}$$

6) Latency computation: The latency $\tau_{j,m}$ for the message m upon reception by VUE j is computed as,

$$\tau_{j,m} = \begin{cases} \sum_{t \in \mathcal{S}} t W_{j,m,t} - t_m^{\mathrm{gen}}, & \text{if } \sum_{t \in \mathcal{S}} W_{j,m,t} \geq 1, \\ \infty, & \text{otherwise.} \end{cases} \tag{23}$$

we have adopted the convention that $\tau_{j,m} = \infty$ if message m is never scheduled for transmission in an RB with SINR greater or equal to γ^{T}.

7) Age of information computation: Let variable $A_{i,j,t} \in \mathbb{R}^+$ indicate the age of information of the messages from VUE i to VUE j at the end of timeslot t. With the assumption of successful reception upon satisfying the SINR threshold γ^{T}, the variable $A_{i,j,t}$ can be computed for $t = 0, 1, \ldots, T-1$ as

$$A_{i,j,t} = \min_{m \in \mathcal{M}_i} (1 + t + A_{i,j}^{\mathrm{init}} - (t_m^{\mathrm{gen}} + A_{i,j}^{\mathrm{init}}) \sum_{t'=0}^{t} W_{j,m,t'}), \tag{24}$$

[1]To disable multihop (i.e., relaying of messages), we replace (22) with the constraint $X_{i,m,f,t} \leq \bigvee_{t'=0}^{t} \Omega_{i,m,t'}$

where the parameter $A_{i,j}^{\text{init}}$ is the initial AoI for before the start of the scheduling interval, i.e., at the beginning of timeslot $t = 0$. For a typical objective function of $A_{i,j,t}$, the above equation can be translated into a set of linear constraints using the method explained in Appendix A-C, where $A_{i,j,t}$ can be thought of as y and $(1+t+A_{i,j}^{\text{init}}-(t_m^{\text{gen}}+A_{i,j}^{\text{init}})\sum_{t'=0}^{t} W_{j,m,t'})$ can be thought of as z_i in (66b) .

B. Latency and AoI Requirements

It should be noted that $\tau_{j,m}$ and $A_{i,j,t}$ is the latency and AoI, respectively, if the messages that are delivered error-free to VUE j and the corresponding delivery times are exactly those indicated by $W_{j,m,t}$. In practice, however, there will be random message errors and the actual latency $\tau_{j,m}^{\text{E}}$ and actual AoI $A_{i,j,t}^{\text{E}}$ will therefore be random. Hence, it is meaningful to formulate probabilistic requirements on the latency and AoI.

The probablistic latency requirement can be formulated as

$$\Pr\{\tau_{j,m}^{\text{E}} \leq \tau^{\text{T}}\} \geq P_{\tau}^{\text{req}} \tag{25}$$

where τ^{T} is the maximum allowed latency (also known as the deadline) and P_{τ}^{req} is the required probability. The probabilistic requirement (25) is guaranteed to be satisfied if (a) message m is scheduled to arrive with latency less or equal to τ^{T} and (b) the end-to-end error probability ϵ^{e2e} for the transmission of message m is small enough: $(1-\epsilon^{\text{e2e}}) \geq P_{\tau}^{\text{req}}$.

As shown in Appendix B-B, we adjust the SINR threshold γ^{T} such that the end-to-end error probability ϵ^{e2e} for all scheduled end-to-end connections is upper bounded by a given requirement ϵ^{req}. To satisfy the probabilistic latency requirement, we use $\epsilon^{\text{req}} = 1 - P_{\tau}^{\text{req}}$.

To summarize, the probabilistic latency requirement (25) is satisfied if

$$\tau_{j,m} \leq \tau^{\text{T}} \tag{26a}$$
$$\epsilon^{\text{req}} = 1 - P_{\tau}^{\text{req}}. \tag{26b}$$

Similarly, the AoI requirement can be formulated, with slight abuse of notation, as

$$\Pr\{\mu(A_{i,j,t}^{\text{E}}) \leq \mu^{\text{T}}\} \geq P_{A}^{\text{req}} \tag{27}$$

where the metric μ is a mapping from $(A_{i,j,t}^{\text{E}} : t \in \mathcal{S})$ to $\mathbb{R}$, μ^{T} is the metric threshold, and P_{A}^{req} is the required probability. Without any essential loss of generality, we will limit our attention to metrics μ such that if $A'_{i,j,t} \leq A_{i,j,t}$, $\forall\, t \in \mathcal{S}$, then $\mu(A'_{i,j,t}) \leq \mu(A_{i,j,t})$. Examples of such metrics is the time average

$$\mu(A_{i,j,t}) = \frac{1}{T}\sum_{t\in\mathcal{S}} A_{i,j,t} \tag{28}$$

and time maximum

$$\mu(A_{i,j,t}) = \max_{t\in\mathcal{S}} A_{i,j,t}. \tag{29}$$

As shown in Appendix C, the probabilistic AoI requirement (27) is satisfied if

$$\mu(A_{i,j,t}) \leq \mu^{\text{T}} \tag{30a}$$
$$\Rightarrow \qquad \epsilon^{\text{req}} \leq 1 - (P_{A}^{\text{req}})^{1/|\mathcal{M}_i|} \tag{30b}$$

where, as usual, ϵ^{req} determines γ^{T} (see (72)).

To conclude, we have shown how to translate probabilistic requirements on latency and AoI into the corresponding deterministic requirements augmented with appropriate requirements on the end-to-end error probability. In the following, we can therefore propose and study RRM algorithms that aim to satisfy deterministic requirements.

C. Basic Problem Formulations

In this section, we will formulate the scheduling and power control problem as MBLP problems for various objectives. The output of the optimization problems is therefore the schedule and power allocation matrices, $\mathbf{X}^{\star}$ and $\mathbf{P}^{\star}$, that optimize the objective function under the specified constraints. Input to the optimization problems is the slow CSI $H_{i,j}$, the set of VUE $\mathcal{N}$, the intended receiver set $\mathcal{R}_i$ for each VUE i, the message generation indicator $\Omega_{i,m,t}$, the ACIR function λ_r, the max power constraint $P^{\max}$, and the SINR threshold γ^{T}. We recall that these variables are needed for $i \in \mathcal{N}$, $j \in \mathcal{N}$, $m \in \mathcal{M}$, $t \in \mathcal{S}$, and $r \in \mathcal{F}$.

We recall that $W_{j,m,t} = 1$ implies that message m is scheduled to arrive at VUE j for the first time in timeslot t. The message will actually be delivered with a probability of at least $(1-\epsilon^{\text{req}})$. Hence,

$$(1-\epsilon^{\text{req}}) \sum_{m\in\mathcal{M}_i}\sum_{t\in\mathcal{S}} W_{j,m,t} \tag{31}$$

is a lower bound on the throughput (i.e., the expected number of unique delivered messages in T timeslots) from VUE i to VUE j . With a slight abuse of terminology, we will call $\sum_{m\in\mathcal{M}_i}\sum_{t\in\mathcal{S}} W_{j,m,t}$ "throughput" in problem formulations 1) and 2) below.

1) Maximizing throughput: The problem to maximize the total sum-throughput of the network can be formulated as

$$\max_{\mathbf{P},\mathbf{X},\mathbf{Y},\mathbf{W}} \sum_{i\in\mathcal{N}}\sum_{j\in\mathcal{R}_i}\sum_{m\in\mathcal{M}_i}\sum_{t\in\mathcal{S}} W_{j,m,t} \tag{32a}$$
subject to,
(9), (10), (11), (19), (21), (22)

2) Maximizing the worst-case throughput: The problem to maximize the minimum throughput of an end-to-end connection in the network can be formulated as

$$\max_{\mathbf{P},\mathbf{X},\mathbf{Y},\mathbf{W}} \eta^{\min} \tag{33a}$$
subject to,
$$\sum_{m\in\mathcal{M}_i}\sum_{t\in\mathcal{S}} W_{j,m,t} \geq \eta^{\min}, \qquad i \in \mathcal{N}, j \in \mathcal{R}_i \tag{33b}$$
(9), (10), (11), (19), (21), (22)

3) Maximizing the connectivity: VUE i and VUE j are said to be connected if at least one message can be sent from i to j with the required end-to-end error probability during the scheduling interval. Let $Z_{i,j} \in \{0,1\}$ indicate that VUE i and j are connected, then

$$Z_{i,j} = \min\Big\{1, \sum_{j\in\mathcal{R}_i}\sum_{m\in\mathcal{M}_i}\sum_{t\in\mathcal{S}} W_{j,m,t}\Big\} \tag{34}$$

Hence, the following problem maximizes the network connectivity[2],

$$\max_{\mathbf{W},\mathbf{X},\mathbf{Y},\mathbf{P},\mathbf{Z}} \sum_{i\in\mathcal{N}} \sum_{j\in\mathcal{R}_i} Z_{i,j} \tag{35a}$$

subject to,

$$Z_{i,j} \le \sum_{t=0}^{T-1} \sum_{j\in\mathcal{R}_i} \sum_{m\in\mathcal{M}_i} W_{j,m,t}, \qquad \forall i,j \in \mathcal{R}_i \tag{35b}$$

$$Z_{i,j} \le 1 \tag{35c}$$

$$(9), (10), (11), (12), (13), (19), (21), (22)$$

Note that, we can formulate the problem to maximize the minimum connectivity for a VUE in the network, i.e., $\max(\min_{i\in\mathcal{N}} \sum_{j\in\mathcal{R}_i} Z_{i,j})$, by a similar transformation as in (33).

4) Maximizing connectivity for AoI requirements: Suppose γ^{T} is chosen such that (30b) is satisfied, then the following problem will maximize the number of end-node pairs (i,j) such that the probabilistic AoI requirement (27) is satisfied:

$$\max_{\mathbf{P},\mathbf{X},\mathbf{Y},\mathbf{W},\mathbf{Z}} \sum_{i\in\mathcal{N}} \sum_{j\in\mathcal{R}_i} Z^{\mathrm{A}}_{i,j} \tag{36a}$$

subject to,

$$\mu(A_{i,j,t}) \le \mu^{\mathrm{T}} + \zeta(1 - Z^{A}_{i,j}), \qquad i\in\mathcal{N}, j\in\mathcal{R}_i \tag{36b}$$

$$Z^{A}_{i,j} \in \{0,1\} \quad \forall i,j \tag{36c}$$

$$(9), (10), (11), (19), (21), (22), (24)$$

The $Z^{A}_{i,j} = \mathbb{1}\{\mu(A_{i,j,t}) \le \mu^{\mathrm{T}}\}$ indicates if the deterministic AoI requirement is satisfied for the end-node pair (i,j) and $\zeta \in \mathbb{R}$ is chosen large enough such that (36b) holds when $Z^{A}_{i,j} = 0$. Clearly, if $\mu(A_{i,j,t}) \le \mu^{\max}$, then $\zeta = \mu^{\max} - \mu^{\mathrm{T}}$ is sufficient. For instance, if $\mu(A_{i,j,t}) = \max_{t\in\mathcal{S}} A_{i,j,t}$, then $\zeta = T + \max_{i\in\mathcal{N},j\in\mathcal{R}_j} A^{\mathrm{init}}_{i,j} - \mu^{\mathrm{T}}$ is sufficiently large.

Problem (36) is an MBLP if (36b) can be translated into a number of linear constraints. This is possible since typically μ is a linear or one-to-one mapping, or if $\mu(A_{i,j,t}) = \max_{t\in\mathcal{S}} A_{i,j,t}$ [3].

5) Maximizing connectivity for latency requirement: To formulate a problem that maximizes the number of end-node pairs (i,j) such that the probabilistic latency requirement (25) is satisfied follows the same logic as for AoI. Suppose γ^{T} is chosen such that (26b) is satisfied, then the following problem will achieve the end goal:

$$\max_{\mathbf{P},\mathbf{X},\mathbf{Y},\mathbf{W},\mathbf{Z}} \sum_{i\in\mathcal{N}} \sum_{j\in\mathcal{R}_i} Z^{\tau}_{i,j} \tag{37a}$$

subject to,

$$\tau_{j,m} \le \tau^{\mathrm{T}} + \zeta(1 - Z^{\tau}_{i,j}), \quad i\in\mathcal{N}, j\in\mathcal{R}_i, m\in\mathcal{M}_i \tag{37b}$$

$$Z^{\tau}_{i,j} \in \{0,1\} \quad \forall i,j \tag{37c}$$

$$(9), (10), (11), (19), (21), (22), (23)$$

where $Z^{\tau}_{i,j} = \mathbb{1}\{\tau_{j,m} \le \tau^{\mathrm{T}}\}$ indicates if the deterministic latency requirement is satisfied for the end-node pair (i,j) and ζ is chosen large enough such that (37b) is holds when $Z^{\tau}_{i,j} = 0$. A technical problem arise here, since, by convention, $\tau_{j,m} = \infty$ if message m is not scheduled to be transmitted in an RB where the SINR at VUE j is larger or equal to γ^{T}. We can resolve this technicality in (23) by replacing ∞ by a very large number, say 10^{10}, and set ζ to the same number. (In a practical implementation with finite-precision arithmetic, more reasonable numbers must, of course, be used.)

D. Variations of Basic Problem Formulations

We note that all of the problem formulations in Section III-C can be made to power control alone problem by fixing $X_{i,m,f,t}$ and to scheduling alone problem by modifying (11) to $P_{i,f,t} = \bar{P}_{i,t}\tilde{X}_{i,f,t}$, where $\bar{P}_{i,t}$ is the transmit power of VUE i if scheduled in timeslot t. Under the assumption that all VUEs use the same transmit power, $\bar{P}_{i,t} = \bar{P}_t$ for all i, then $\bar{P}_t = P^{\max}$ maximizes the performance for all scheduling alone algorithms, as proved in [10]. The resulting problems are MBLP and Boolean linear programming (BLP) problems, respectively.

Moreover, scheduling and power control can be done for certain subset of timeslots alone. Assume that we are interested in scheduling and power control on and after timeslot $T' < T$ only, and we know the packet reception status for all the timeslots prior to timeslot T'. Then we can set all variables (i.e., $\mathbf{P},\mathbf{X},\mathbf{Y},\mathbf{W}$) corresponding to timeslots $\{0,1,\ldots,T'-1\}$, and optimize over all variables corresponding to timeslots $\{T',T'+1,\ldots,T\}$. This way, we can accommodate the information upon any past transmissions and AoI. For instance, the scheduling and power control can be done for all timeslots one by one, to reduce computational complexity. Other practical considerations such as supporting large message payload and high reliability, are discussed in Appendix B.

IV. Clustering of Network

The basic problem formulations in Section III-C have computational complexities that scale poorly with the network size N. To address this issue, we propose to partition the network into smaller groups and perform resource allocation in each group independently.

The clustering and grouping mechanism is illustrated in Fig. 3. The entire network is partitioned into C clusters and each cluster into G groups. A group g in cluster c is called group (c,g). The notion of a group is similar to a cell in a

[2]We do not need to explicitly constrain $Z_{i,j}$ to be boolean, since $Z_{i,j}$ is upper bounded by an integer that is nonnegative and at most equal to 1, i.e, constraints (35b) and (35c), respectively. This would reduce computational complexity as shown in Section VI.

[3] If μ is a linear map, then obviously (36b) is a linear constraint. Similarly, if $\mu(A_{i,j,t}) = \max_{t\in\mathcal{S}} A_{i,j,t}$, then (36b) can be translated into a set of linear constraints $A_{i,j,t} \le \mu^{\mathrm{T}} + \zeta(1 - Z^{A}_{i,j})$, for $i\in\mathcal{N}, j\in\mathcal{R}_i, t\in\mathcal{S}$.

Next, we prove linearity of (36b) when μ is a one-to-one mapping. Without much loss of generality, we assume that μ is a non-decreasing function (a similar line of proof holds for non-increasing μ function as well). Then (36b) can be translated to $A_{i,j,t} \le \mu^{-1}(\mu^{\mathrm{T}} + \zeta(1 - Z^{A}_{i,j}))$, for $i\in\mathcal{N}, j\in\mathcal{R}_i, t\in\mathcal{S}$, where μ^{-1} is the inverse function of μ. Since $Z^{A}_{i,j} \in \{0,1\}$, this constraint is equivalent to the linear constraint $A_{i,j,t} \le \tilde{\mu}^{\mathrm{T}} + \tilde{\zeta}(1 - Z^{A}_{i,j})$, where $\tilde{\mu}^{\mathrm{T}} = \mu^{-1}(\mu^{\mathrm{T}})$ and $\tilde{\zeta} = \mu^{-1}(\mu^{\mathrm{T}} + \zeta) - \tilde{\mu}^{\mathrm{T}}$.

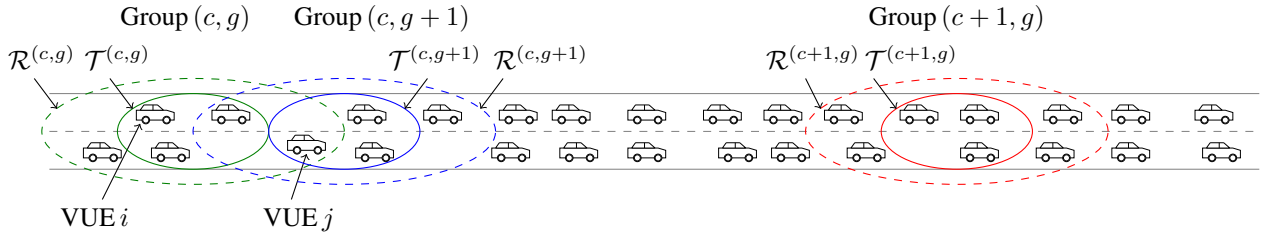

Fig. 3: Groups (c,g) and $(c+1,g)$ are separated by more than the reuse distance and can therefore reuse timeslots.

traditional cellular system. The available time slots will be partitioned among the groups belonging to a cluster, which will eliminate intergroup interference since groups (c,g) and (c,g'), will use nonoverlapping timeslots when $g' \neq g$. We can therefore do scheduling and power control for each group in a cluster independently, which greatly reduces the computational complexity as the network size N decreases.

However, since groups (c,g) and (c',g) can use the same timeslots, there will in general be intercluster interference. It is therefore important to design the clusters and groups such that this interference is limited. In the following, we will propose a method for this.

We start by defining some notation. Let $\mathcal{T}^{(c,g)} \subseteq \mathcal{N}$ denote the set of Tx-VUEs in group (c,g) for $c = 0,1,\ldots,C-1$ and $g = 0,1,\ldots,G-1$. Moreover, let

$$\mathcal{R}^{(c,g)} = \{j : i \in \mathcal{T}^{(c,g)},\, j \in \mathcal{R}_i\} \tag{38}$$

be the set of Rx-VUEs intended to receive messages from VUEs in group (c,g).

We note that the transmitter groups form a partitioning of the network, i.e., $\mathcal{T}^{(c,g)} \cap \mathcal{T}^{(c',g')} = \emptyset$ for $(c,g) \neq (c',g')$ and the union of all transmitter groups contains all N VUEs. However, the Rx-VUE sets $\mathcal{R}^{(c,g)}$ can be overlapping, as shown in Fig. 3.

A. 1-Hop Feasibility

Consider the link (i,j) between VUE i and VUE j. If the channel gain $H_{i,j}$ is large enough to allow for direct (one-hop) communication with SNR greater or equal to γ^{T}, then we say that the link (i,j) is *1-hop feasible*. If the link is not 1-hop feasible, we must rely on multihop communication (relaying) to connect VUE i and j.

Suppose VUE i is transmitting on RB (f,t). Then the SINR for the link (i,j) can be upper-bounded as

$$\frac{S_{i,j,f,t}}{\sigma^2 + R_{j,f,t} - S_{i,j,f,t}} \leq \frac{S_{i,j,f,t}}{\sigma^2} \leq \frac{P^{\max} H_{i,j}}{\sigma^2}. \tag{39}$$

Clearly, the link (i,j) is 1-hop feasible only if

$$H_{i,j} \geq \gamma^{\mathrm{T}} \sigma^2 / P^{\max}, \tag{40}$$

and we define the set of receivers to VUE i that are 1-hop feasible as

$$\mathcal{D}_i \triangleq \{j \in \mathcal{N} : H_{i,j} \geq \gamma^{\mathrm{T}} \sigma^2 / P^{\max}\}. \tag{41}$$

Note that we are considering all VUEs as potential receivers in the definition of $\mathcal{D}_i$, not only the receivers in $\mathcal{R}_i$, since we want to consider also the case when VUE i relays messages to VUEs that are not in $\mathcal{R}_i$ (its set of intended end receivers). We note that the set of VUEs that can be reached by a VUE in $\mathcal{T}^{(c,g)}$ is

$$\mathcal{D}^{(c,g)} = \bigcup_{i \in \mathcal{T}^{(c,g)}} \mathcal{D}_i. \tag{42}$$

B. Reuse Distance and Clustering

While clustering, we want to limit the intercluster interference to the receivers in $\mathcal{D}_i$ for all i. There will be no intergroup interference within a cluster, since distinct groups will use nonoverlapping timeslots. However, timeslots are reused among clusters, i.e., transmitters in the same group but different clusters can use the same timeslot. Suppose $i \in \mathcal{T}^{(c,g)}$, then the intercluster interference to receiver $j \in \mathcal{D}_i$ is

$$\begin{aligned}
&\sum_{\substack{k \in \mathcal{T}^{(c',g)} \\ c' \neq c}} \sum_{f'=0}^{F-1} \tilde{X}_{k,j,f',t} P_{k,j,f',t} H_{k,j} \lambda_{|f'-f|} \\
&\qquad \leq \sum_{\substack{k \in \mathcal{T}^{(c',g)} \\ c' \neq c}} \sum_{f'=0}^{F-1} P^{\max} H_{k,j} \lambda_{|f'-f|} && \text{(43a)} \\
&\qquad \approx \sum_{\substack{k \in \mathcal{T}^{(c',g)} \\ c' \neq c}} P^{\max} H_{k,j} && \text{(43b)} \\
&\qquad \lessapprox 2P^{\max} \max_{\substack{k \in \mathcal{T}^{(c',g)} \\ c' \neq c}} H_{k,j} && \text{(43c)}
\end{aligned}$$

where in the first approximation (43b), we have assumed the worst-case CCI (max power and CCI from all clusters) and ignored the ACI. This is because ACI is negligible compared to CCI, i.e., $\sum_{f'=0,f' \neq f}^{F-1} \lambda_{|f'-f|} \ll \lambda_0 = 1$ for a typical ACIR model λ. In the second approximation (43c), we ignore CCI from non-neighbouring clusters and upper bound the CCI from the neighbouring clusters. This is because non-neighbouring clusters cause significantly less interference compared to neighbouring clusters, due to the high penetration loss of intermediate VUEs. In other words, we ignored all CCI terms except the two largest terms (corresponding to the two neighbouring clusters) and then replaced the second largest term with the largest term (resulting in the factor 2).

Algorithm 1 Clustering Algorithm

Input: $\{N, \mathbf{H}, \delta, \sigma^2, P^{\max}, N^{\mathrm{Tx}}\}$
Output: $C, G, \mathcal{T}^{(c,g)}, \mathcal{R}^{(c,g)}, \mathcal{S}_g$
1: Compute G using (45) and (47)
2: Compute C using (48).
3: Compute $\mathcal{T}^{(c,g)}$ and $\mathcal{R}^{(c,g)}$, $\forall (c,g)$ using (49) and (38)
4: Compute $\mathcal{S}_g$, $\forall g$ using (50)

While clustering, we strive to set the reuse distance sufficiently large such that the intercluster interference does not exceed $\delta\sigma^2$ from some (small) δ. Using the approximation (43c), we can achieve this if

$$H_{k,j} \leq \frac{\delta\sigma^2}{2P^{\max}}, \quad i \in \mathcal{T}^{(c,g)}, j \in \mathcal{D}_i, k \in \mathcal{T}^{(c',g)}, c' \neq c, \forall g. \tag{44}$$

Assuming VUEs are indexed based on their position, we ensure (44) by setting $|k-i| > d^{\text{reuse}}$ for all VUEs i and k that belong to the same group but different clusters, where

$$d^{\text{reuse}} = \max_{i \in \mathcal{N}, k \in \mathcal{N}} \big\{ |k-i| : H_{k,j} > \frac{\delta\sigma^2}{2P^{\max}}, j \in \mathcal{D}_i \big\}. \tag{45}$$

Clustering and grouping can be done in any arbitrary manner, however, must satisfy the following condition,

$$|k-i| \geq d^{\text{reuse}} \; \forall \, i \in \mathcal{T}^{(c,g)}, \; k \in \mathcal{T}^{(c',g)}, c' \neq c \tag{46}$$

For the sake of simplicity, we explain our RRM algorithm for a simple clustering and grouping scheme where each group has the same number of VUEs N^{Tx}, and each cluster contains at least $\lceil N^{\mathrm{Tx}} + d^{\text{reuse}} \rceil$ VUEs. Indeed such a clustering and grouping scheme satisfies the condition (46). Since each group is utilizing the same number of resources, it would be favourable to have same number of VUEs in each group. Additionally, this also allows radio resource reuse on every fixed distance for certain vehicular topologies, e.g., a dense traffic scenario topology where adjacent vehicular distances are approximately equal [51]. However, we note that our RRM algorithms are not limited by this particular clustering and grouping scheme.

Following this, we can compute the number of groups G and the number of clusters C as follows,

$$G = \left\lceil \frac{N^{\mathrm{Tx}} + d^{\text{reuse}}}{N^{\mathrm{Tx}}} \right\rceil \tag{47}$$

$$C = \left\lceil \frac{N}{GN^{\mathrm{Tx}}} \right\rceil \tag{48}$$

We can now form the group (c,g) for $c = 0, 1, \ldots, C-1$ and $g = 0, 1, \ldots, G-1$ as

$$\mathcal{T}^{(c,g)} = \{(cG+g)N^{\mathrm{Tx}} + n : n = 0, 1, \ldots, N^{\mathrm{Tx}} - 1\}, \tag{49}$$

and $\mathcal{R}^{(c,g)}$ follows from (38). We will assign the the timeslots in $\mathcal{S}_g$ to group (c,g), where

$$\mathcal{S}_g \triangleq \{g + \ell G : g + \ell G < T, 0 \leq \ell \leq \lfloor T/G \rfloor\} \tag{50}$$

The clustering procedure is summarized in Algorithm 1.

C. Scheduling and Power Control

As mentioned above, we can perform scheduling and power control for each group independently. The required computations can be done in a completely centralized fashion by a single controller or be distributed to at most CG controllers, one per group in the network. Hybrids of these extreme architectures are, of course, also possible. The controllers can be hosted by fixed infrastructure nodes (e.g., in BSs or edge computing devices) or by specially assigned VUEs.

All problem formulations in Section III-C can used to compute the schedule and power control for a particular group after the following modifications.

Firstly, we need to modify the SINR constraint (19) to add a margin for the inter-cluster interference,

$$S_{i,j,f,t} \geq \bar{\gamma}^{\mathrm{T}}(\sigma^2(1+\delta) + R_{j,f,t}) - \zeta(1 - Y_{i,j,f,t}). \tag{51}$$

Secondly, we reduce the matrices $\mathbf{P}$, $\mathbf{X}$, $\mathbf{Y}$, $\mathbf{W}$, and $\mathbf{Z}$ and limit the input variables $H_{i,j}$ and $\Omega_{i,m,t}$ to cover only the relevant variables for the group. In general, we need to consider only the transmitters $i \in \mathcal{T}^{(c,g)}$, receivers $j \in \mathcal{R}^{(c,g)}$, messages $m \in \mathcal{M}^{(c,g)} = \cup_{i \in \mathcal{T}^{(c,g)}} \mathcal{M}_i$, and timeslots $t \in \mathcal{S}^g$.

In particular, this will reduce the dimensions of the matrices such that

$$\mathbf{P} \in \{0,1\}^{N^{\mathrm{Tx}} \times F \times T_g}, \tag{52}$$

$$\mathbf{X} \in \{0,1\}^{N^{\mathrm{Tx}} \times M \times F \times T_g}, \tag{53}$$

$$\mathbf{Y} \in \{0,1\}^{N^{\mathrm{Tx}} \times N_g^{\mathrm{Rx}} \times F \times T_g}, \tag{54}$$

$$\mathbf{W} \in \{0,1\}^{N_g^{\mathrm{Rx}} \times M_g \times T_g}, \tag{55}$$

$$\mathbf{Z} \in \{0,1\}^{N_g^{\mathrm{Rx}} \times N_g^{\mathrm{Rx}}}, \tag{56}$$

where $T_g = |\mathcal{S}_g|$, $N_g^{\mathrm{Rx}} = |\mathcal{R}^{(c,g)}|$, and $M_g = |\mathcal{M}^{(c,g)}|$.

The main advantage with clustering is a reduction of the overall computational complexity (see Section VI). The main drawbacks is (a) a potential loss of performance (since clustering cannot improve the optimal values of objective functions) and (b) that multihop communication (relaying) is only possible between end-nodes $i \in \mathcal{T}^{(c,g)}$ and $j \in \mathcal{D}^{(c,g)}$. Hence, any intended receiver $j \in \mathcal{R}^{(c,g)} \backslash \mathcal{D}^{(c,g)}$ cannot receive any messages.

Within the current framework, such connections can only be enabled by relaying through the fixed infrastructure, i.e., the messsage is transmitted from the source VUE i via an uplink to its serving base station (BS), which in turn forwards the message to a base station that can reach the destination VUE j via a downlink. This will, require some (minor) modifications of the basic framework in this paper, incur extra latency that might not be acceptable, and will only work when VUEs are inside coverage of the fixed network infrastructure. Finding a better relaying strategy for long connections is, however, outside the scope of this paper. We also note that this problem is most prevalent when the source and destination VUEs are far from each other and the source at the edge of the group. Hence, the problem might not be so serious, since most traffic safety applications with low latency requirements rely on communication over relative short distances.

Algorithm 2 CDS

Input: $\{i', N^{\mathrm{Tx}}, T, F, G, \beta, \lambda\}$
Output: $\tilde{\mathbf{X}}$

$\tilde{\mathbf{X}} = \mathbf{0}^{N^{\mathrm{Tx}} \times F \times T}$
$\mathcal{J} = \mathcal{T}^{(c,g)}$ // unscheduled VUEs
$\mathcal{U} = \{(f,t) : f \in \mathcal{F}, t \in \mathcal{S}_g\}$ // unscheduled RBs
$c = \lfloor i'/(GN^{\mathrm{Tx}}) \rfloor$
$g = \lfloor i'/N^{\mathrm{Tx}} \rfloor \bmod G$
Compute $\mathcal{T}^{(c,g)}$ from c, g, and N^{Tx} using (49)
Compute $\mathcal{S}_g$ from g, T, and G using (50)
// Stage 1: Schedule all VUEs in group (c,g) exactly once
do
  $(i^*, f^*, t^*) = \underset{\{(i,f,t): i \in \mathcal{J}, (f,t) \in \mathcal{U}\}}{\arg\min} \sigma_I^2(i, f, t; \tilde{\mathbf{X}})$
  $\tilde{X}_{i^*,f^*,t^*} = 1$
  $\mathcal{J} = \mathcal{J} \setminus \{i^*\}$
  $\mathcal{U} = \mathcal{U} \setminus \{(f^*, t^*)\}$
while $\mathcal{J} \neq \emptyset$
// Stage 2: Allocate remaining unscheduled RBs
for $(f,t) \in \mathcal{U}$ **do**
  $i^* = \underset{i \in \mathcal{T}^{(c,g)}: \vee_{f'=0}^{F-1} \tilde{X}_{i,f',t} = 0}{\arg\min} \sigma_I^2(i, f, t; \tilde{\mathbf{X}})$
  $\tilde{X}_{i^*,f,t} = 1$
end for

V. Clustering-Based Distributed Scheduling (CDS)

The RRM solutions described above are centralized in the sense that the computation of the schedule and power allocation is performed by a central controller (e.g., a BS or a specially elected VUE). In this section, we will present a cluster-based scheduling algorithm that is fully distributed. That is, a scheme in which each VUE computes its group schedule, independently of the other VUEs. The algorithm, called clustering-based distributed scheduling (CDS), requires knowledge of the position index i' of an arbitrary VUE in the group, the system parameters T, F, N^{Tx}, G, and the ACIR function λ. The algorithm has also a tuning parameter β, which is described below. It should be noted that CDS does not require the channel state matrix $\mathbf{H}$. The output is the scheduling matrix $\mathbf{X}$, which can be used with any power matrix. Hence, power values can be assigned to all VUEs in any manner before/after CDS algorithm.

The rationale behind the algorithm is based on the assumption that each VUE would like to transmit messages to its nearby VUEs [1]. Hence, the interference the *transmitter* VUE i experiences is approximately equal to the interference its intended *receiver* VUE j, $j \in \mathcal{R}_i$, experiences. Hence, it makes sense to schedule the VUE i *transmission* on an RB (f,t) where VUE i would experience low *received* interference. Since the interference depends on the schedule, we construct the schedule in an iterative, greedy fashion. However, it is worth mentioning that the CDS algorithm does not assume any of the above rationales to be true, and, hence, CDS can be applied in any scenario (with varying performance, of course).

To be more precise, we have at the beginning of an iteration access to the partial schedule $\tilde{\mathbf{X}}$ constructed so far. The intragroup interference that VUE $i \in \mathcal{T}^{(c,g)}$ experiences in RB (f,t) is

$$\sum_{k \in \mathcal{T}(c,g)} \sum_{f' \in \mathcal{F}} \bar{P}_{k,f',t} \tilde{X}_{k,f',t} H_{k,i} \lambda_{|f'-f|} \tag{57}$$

where $\bar{P}_{k,f',t}$ is the transmit power of VUE k if scheduled in RB (f',t). Ignoring pathloss and assuming that each blocking vehicle introduce an additional gain $\beta < 1$, we note that $H_{k,i} = \beta^{|k-i|-1}$. Hence, the intragroup interference is proportional to

$$\sigma_I^2(i, f, t; \tilde{\mathbf{X}}) \triangleq \sum_{k \in \mathcal{T}(c,g)} \sum_{f' \in \mathcal{F}} \tilde{X}_{k,f',t} \lambda_{|f'-f|} \beta^{|k-i|-1}. \tag{58}$$

The main idea is to iteratively identify the triplet (i^*, f^*, t^*) that minimizes $\sigma_I^2(i, f, t; \tilde{\mathbf{X}})$ (under some suitable constraints) and schedule VUE i^* in RB (f^*, t^*). The process is then repeated until a termination criterion is met.

We propose to construct the schedule in three steps. In the first step, we ensure that each VUE in the group is scheduled exactly once. In the second step, we assign any unscheduled RBs to the VUEs in the group (without attempting to keep the number of RBs assigned equal for all VUEs). In the third step, we assign messages to the scheduled RBs.

For simplicity, we describe the algorithm for the case when all VUEs have exactly one own message to transmit during the scheduling interval and that this message is available at timeslot $t = 0$. The extension to a more general data traffic model is not difficult, but would complicate the presentation here.

The first two steps are summarized in Alg. 2, which outputs $\tilde{\mathbf{X}}$. Ties in the $\arg\min$ operations in Alg. 2 are resolved to the smallest value of i, f, and t. Due to this, the VUE with the lowest index in the group will be scheduled in RB $(0,g)$, the second lowest VUE will be scheduled in $(0, g+G)$, etc. Once all timeslots in $\mathcal{S}_g$ been scheduled once, VUEs will start to be multiplexed in frequency. Note that, a VUE is scheduled at most once in a timeslot to avoid sharing of transmit power among RBs in a timeslot.

What remains is the third step: to assign messages indices to the scheduled transmissions, i.e., convert $\tilde{X}_{i,f,t}$ to $X_{i,m,f,t}$. This can be done in many ways. At a scheduled RB (f,t), the VUE can choose to transmit its own message or transmit (i.e., relay) any other message that was received at or before timeslot $\lceil t - t^{\mathrm{p}} \rceil$. A reasonable strategy is for each VUE to (a) transmit is own message at the earliest scheduled timeslot, and (b) for any future scheduled timeslots, relay a message that was received from the furthest located VUE. Messages are only relayed once, and if no message is available for relaying, the VUE transmits its own message again. Rule (a) strives to disseminate the original messages as quickly as possible inside the group, and rule (b) strives to relay messages as far as possible for each hop.

VI. Computational Complexity Analysis

In general, the worst case complexity of an MBLP problem with m Boolean variables and n continuous variables can be upper-bounded as $\mathcal{O}(\frac{n^3 2^m}{\log n})$. The complexity 2^m is for fixing m Boolean variables, and the complexity $\frac{n^3}{\log n}$ is for solving each of the resulting linear programming (LP) problem using an interior point method [52]. Since $\mathbf{X}, \mathbf{Y}, \mathbf{W}$ are Boolean and $\mathbf{P}, \mathbf{Z}$ are continuous variable matrices, we can upper-bound the worst-case computational complexity of all problem formulations with objectives throughput or connectivity as $\mathcal{O}(CG\frac{(|\mathbf{P}|+|\mathbf{Z}|)^3 2^{|\mathbf{X}|+|\mathbf{Y}|+|\mathbf{W}|})}{\log(|\mathbf{P}|+|\mathbf{Z}|)})$, where operation $|\cdot|$ indicate the number of elements in the matrix, and CG account for the total number of groups in the network. Obviously, making $Z_{i,j}$ a continuous variable instead of boolean variable in problem formulation (35) reduces the computational complexity. Similarly for the problem formulation (36) and (37) the complexity are $\mathcal{O}(CG\frac{((|\mathbf{P}|+|\mathbf{A}|)^3 2^{|\mathbf{X}|+|\mathbf{Y}|+|\mathbf{W}|+|\mathbf{Z}^{\mathrm{A}}|})}{\log(|\mathbf{P}|+|\mathbf{A}|)})$ and $\mathcal{O}(CG\frac{((|\mathbf{P}|+|\mathbf{A}|)^3 2^{|\mathbf{X}|+|\mathbf{Y}|+|\mathbf{W}|+|\mathbf{Z}^{\tau}|})}{\log(|\mathbf{P}|+|\mathbf{A}|)})$. Note that the significant computational complexity reduction due to clustering is mainly due to the reduction of the size of matrices as shown in (52)–(56).

For Algorithm 2, there are N^{Tx} iterations in the first stage, and $\max\{0, FT_g - N^{\mathrm{Tx}}\}$ iterations in the second stage. Within an iteration in the first stage, the algorithm has to search through all $N^{\mathrm{Tx}}FT_g$ possible combinations of scheduling, hence, complexity is $\mathcal{O}((N^{\mathrm{Tx}})^2 FT_g)$. Similarly, the computational complexity of second stage is at most $\mathcal{O}(N^{\mathrm{Tx}}FT_g)$. A VUE can transmit maximum FT_g messages, therefore, the worst-case complexity for stage 3 is $\mathcal{O}(N^{\mathrm{Tx}}FT_g)$. In summary, the worst-case complexity of Algorithm 2 is upper-bounded by $\mathcal{O}(N^{\mathrm{Tx}}FT_g(N^{\mathrm{Tx}}+2))$. For the whole network, the complexity is $\mathcal{O}(CGN^{\mathrm{Tx}}FT_g(N^{\mathrm{Tx}}+2)) = \mathcal{O}(NFT_g(N^{\mathrm{Tx}}+2))$, since $CGN^{\mathrm{Tx}} = N$.

VII. Performance Evaluation

A. Scenario and Parameters

The simulation parameters are summarized in Table III. For the simulation purpose, we consider a vehicular platooning scenario, where vehicles are distributed on a convoy in similar to Fig. 3. Platooning is a promising intelligent transport system (ITS) use case that has the potential to increase road capacity, reduce fuel consumption and improve driver comfort [54]–[56]. Furthermore, vehicular platooning is one of the four enhanced V2X scenarios as per 3GPP [1]. However, note that the proposed algorithms do not assume any particular network topology or simulation parameter values.

The distance d between any two adjacent VUEs is modeled as a shifted exponential distributed random variable, with minimum distance $d_{\min}$ and average distance d_{avg} [51], [57]–[59]. That is, in each trial of the simulation, we drop VUEs in a convoy with random adjacent vehicular distances d, whose probability density function is given as,

$$f(d) = \begin{cases} (d_{\text{avg}} - d_{\min})^{-1} \exp(-\frac{d-d_{\min}}{d_{\text{avg}}-d_{\min}}), & d \geq d_{\min} \\ 0, & \text{otherwise} \end{cases} \quad (59)$$

TABLE III: System Simulation Parameters

Parameter	Value
Duplex mode	Half-Duplex
ACIR model	3GPP mask [53]
γ^{T}	7 dB
$P^{\max}$	24 dBm
PL_0	63.3 dB
α	1.77
d_0	10 m
σ_1	3.1 dB
Penetration Loss	10 dB per obstructing VUE
σ^2	-95.2 dBm
δ	$1/100$
d_{avg}	48.6 m
$d_{\min}$	10 m
β	0.1
ζ	$\gamma^{\mathrm{T}}(NP^{\max} + \sigma^2)$
t^{P}	1

where $d_{\text{avg}} = 48.6$ m, corresponding to 2.5 seconds for a vehicular speed of 70 km/h, as recommended by 3GPP [60, section A.1.2] for freeway scenario.

We assume that each VUE wants to broadcast its message within T timeslots to the nearest N^{Rx} VUEs, i.e., $\mathcal{R}_i$ is the closest N^{Rx} VUEs to VUE i. This is in line with CAMs scenario proposed by ETSI, where the message generation is periodic with periodicity T. Furthermore, we set $t^{\mathrm{P}} = 1$, so that the relaying can be done 1 timeslot after the reception. However, note that these T timeslots are allocated to G groups in non-overlapping manner (i.e., each group gets approximately T/G timeslots), and group g gets timeslots $\mathcal{S}_g$ as computed in (50).

ETSI defines V2V platooning scenario having message payloads of 300-400 bytes [1], and the spectrum available for transmission as 5.875–5.905 GHz [61, Table 4.2-1]. The physical layer transmission procedures for V2V sidelink is explained in [62, Section 14]. For simulation purpose, we choose a bandwidth of 10 MHz, which corresponds to 50 RBs in a timeslot. In order to support a message payload of 400 bytes, we set $\gamma^{\mathrm{T}} = 7$ dB, and a VUE is allocated with a contiguous RB-group of 10 RBs each. Indeed, transmitting in 10 RBs with SINR 7 dB achieves sufficiently low error probability for 400 bytes payload. Therefore, in this context, we set the unit of scheduling as RB-Group (consisting of 10 RBs) instead of 1 RB, i.e., we schedule VUEs on each RB-Group instead of RB. This in turn reduces the computational complexity since $F = 5$ instead of 50. Indeed, 3GPP support CSI report and scheduling on RB-groups instead of individual RBs to reduce control overhead.

The channel model and parameters are adopted from [63], which is a model based on V2V link measurements at carrier frequency 5.2 GHz in a highway scenario, and in line with the measurements done in [64]–[66]. The pathloss model is,

$$\mathrm{PL}(d) = \mathrm{PL}_0 + 10\alpha \log_{10}(d/d_0) + X_{\sigma_1} \quad (60)$$

where d is the distance, α is the pathloss exponent, PL_0 is the pathloss at a reference distance $d_0 = 10\,\mathrm{m}$, and X_{σ_1} is the shadowing effect modeled as a zero-mean Gaussian random variable with standard deviation σ_1. The penetration loss caused by a blocking vehicle has been widely measured and observed to be 12-13 dB for a truck [7], 15-20 dB for a bus [9], 20 dB for a van [8], and 10 dB for a car [6]. However, there is a lack of enough measurements for the penetration loss caused by multiple obstructing vehicles. Measurements in [67] shows that the variance of the shadow fading for two blocking VUEs is greater than for one blocking VUE. For the simulation purpose, we assume penetration loss of 10 dB for each obstructing VUE, which might be an over-estimate for the penetration loss. The proposed algorithms assume the knowledge of slowly varying channel. The scheduling time horizon is related to the latency requirement and typically less than 100 ms, over which time the slow channel state information (i.e., pathloss and shadowing) does not vary significantly, even at highway speeds. The noise variance is $-95.2\,\mathrm{dBm}$ and $P^{\max}$ is 24 dBm as per 3GPP recommendations [53]. The $\delta = 0.01$, which implies that the the worst case inter-cluster interference is limited to 1% of the noise power. We note that this value of δ results in $11 \leq d^{\mathrm{reuse}} \leq 13$, consequently, $G = 3$ for $N^{\mathrm{Tx}} = 10$, and $G = 2$ for $N^{\mathrm{Tx}} \geq 20$.

Finally, the ACIR value λ_r is chosen as the mask specified by 3GPP [53], as follows,

$$\lambda_r = \begin{cases} 1, & r = 0 \\ 10^{-3}, & 1 \leq r \leq 4 \\ 10^{-4.5}, & \text{otherwise} \end{cases}. \tag{61}$$

B. Simulation Results

Ideally, we want to consider a vehicular network of a very large size. However, as already mentioned in Section IV, interference is negligible for clusters beyond 2^{nd} neighboring cluster on each side. Therefore, we simulate a network of 5 clusters (i.e., $C = 5$), but analyze the performance of VUEs in the the middle cluster (i.e., 3^{rd}cluster) alone. This is to avoid edge effects, since clusters 1,2,4,5, have less neighbors on one side, hence, unfair to compare.

We set the value of N^{Tx} first, then compute the value of G using (47), and $N = CGN^{\mathrm{Tx}} = 5GN^{\mathrm{Tx}}$ since the number of clusters is fixed to 5. Recall that the number of groups G depends upon N^{Tx} as per (47).

The V2V communication typically does not require very high datarates, and throughput might not be a very important metric. However, connectivity is important for V2V safety-related communication [1]. For this reason, we present simulation results for maximizing connectivity by solving (35), i.e., maximizing the number of receivers that can successfully receive a message from a VUE. However, since each VUE has a single message to multicast in T timeslots, maximizing the connectivity during T timeslots is equivalent to maximizing throughput, i.e., the problem formulations (32) and (35) are equivalent in our simulation scenario. We also note that maximizing connectivity is equivalent to minimizing the average AoI in our simulation scenario.

Fig. 4 and 5 show the simulation results, and the compared algorithms are summarized in Table IV. The last column in Table IV indicates the performance of various algorithms for $N^{\mathrm{Tx}} = 20, N^{\mathrm{Rx}} = 20$, and $T = 12$. To the best of our knowledge, there exists no multicast scheduling algorithm with the objective of maximizing the connectivity in the current literature, except our own previous works. In particular, there are no ACI-aware RRM schemes except the ones we have proposed [10], [11]. To benchmark the algorithms proposed in this paper, we are therefore forced to mainly compare with our own previous schemes. However, we were able to find one multicast scheme in the literature that is relatively close to our setup, namely the one proposed by Peng et al. [68]. We have modified their objective to maximize connectivity instead of maximizing the minimum SINR among the intended links. This allows us to benchmark our algorithms to this modified scheme, shown as the black curves marked with plus in Figs. 4-5. Furthermore, the scheduling algorithms in [10], [68] are centralized algorithms and require CSI between all pairs of VUEs in the network, while CDS is a distributed algorithm without the need of CSI. The algorithms in [10], [68] and CDS have polynomial computational complexity, whereas the joint scheduling and power control problem formulations (i.e., (32)–(37)) have exponential computational complexity. All the simulations are done in Matlab. In order to solve all MBLP and BLP problems, we use Gurobi toolbox [69] in addition to Matlab.

To quantify the gain due to the multihop, we also show the results for joint scheduling and power control after disabling multihop as blue curves with circles in Fig. 4 and 5. The performance gap between (35) with and without multihop shows the significant improvement due to multihop.

In Fig. 4 (a), we plot the average connectivity of a VUE (i.e., $1/|\mathcal{N}| \sum_{i \in \mathcal{N}} \sum_{j \in \mathcal{R}_i} Z_{i,j}$) for various values of group sizes N^{Tx}. The performance improvement for CDS is significant when $N^{\mathrm{Tx}} \leq 20$ since the scheduler has more number of RBs to schedule compared to the number of VUEs (i.e., $FT > N^{\mathrm{Tx}}$), hence can utilize the extra RBs for multihop to enhance the connectivity. We observe an optimality gap of 14.6% for CDS algorithm compared to optimal scheduling with multihop, when $N^{\mathrm{Tx}} = 20, N^{\mathrm{Rx}} = 20$, and $T = 12$. For higher values of N^{Tx}, the performance decreases for CDS, [10] and [68] mainly due to their non-overlapping scheduling nature, i.e., an RB cannot be scheduled to more than one VUE.

As we increase the time-horizon for scheduling T, the performances of all the algorithms improve as seen from Fig. 4 (b). This is not surprising, since more number of timeslots become available for scheduling for each group as we increase T. However, for the scheduling algorithms not supporting multihop, the performance do not improve for higher values of T, since links beyond 3^{rd}neighbor on each side of the transmitting VUE tend to be noise limited, due to the high penetration loss of intermediate VUEs [6]. Fig. 4 (c) shows the performance for various number of

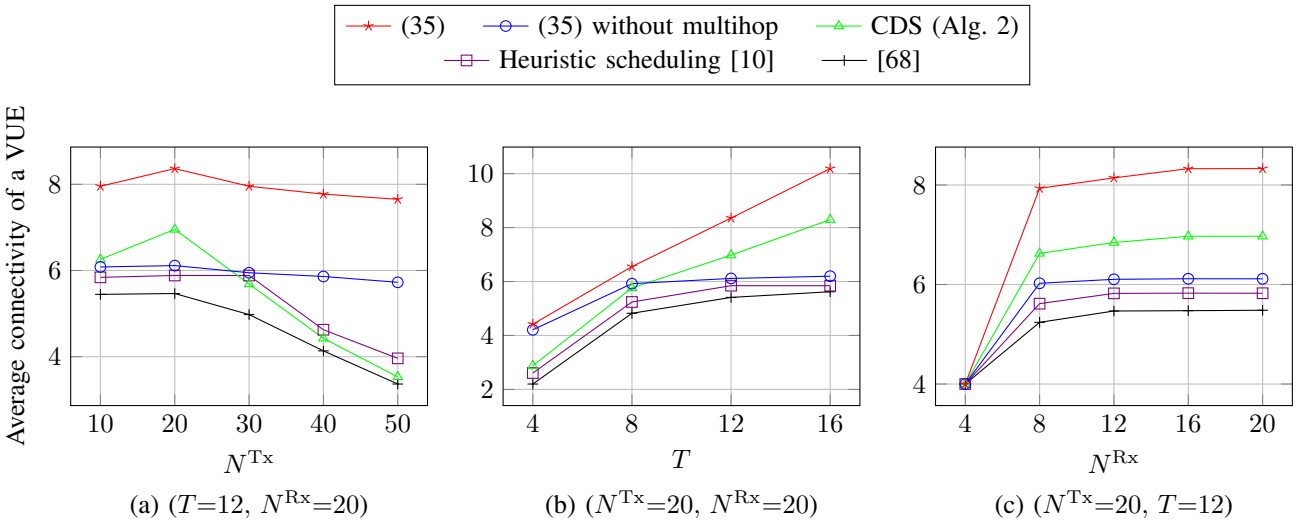

(a) (T=12, N^{Rx}=20) (b) (N^{Tx}=20, N^{Rx}=20) (c) (N^{Tx}=20, T=12)

Fig. 4: Average connectivity of a VUE for various algorithms

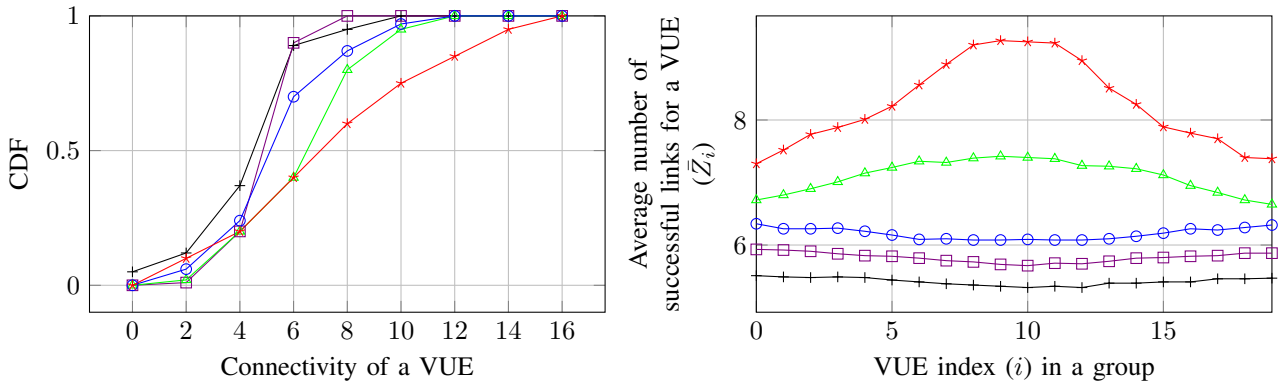

(a) (b)

Fig. 5: Fairness comparison of connectivity of a VUE (N^{Tx}=20, T=12, N^{Rx}=20)

TABLE IV: Summary of compared algorithms

Line Style	Scheduling	Power	Complexity (worst-case)	Algorithm	Average connectivity
★	Optimized	Optimized	$\mathcal{O}(CG\frac{(\lvert\mathbf{P}\rvert+\lvert\mathbf{Z}\rvert)^3 2^{\lvert\mathbf{X}\rvert+\lvert\mathbf{Y}\rvert+\lvert\mathbf{W}\rvert}}{\log(\lvert\mathbf{P}\rvert+\lvert\mathbf{Z}\rvert)})$	(35)	8.37
○	Optimized	Optimized	$\mathcal{O}(CG\frac{(\lvert\mathbf{P}\rvert+\lvert\mathbf{Z}\rvert)^3 2^{\lvert\mathbf{X}\rvert+\lvert\mathbf{Y}\rvert}}{\log(\lvert\mathbf{P}\rvert+\lvert\mathbf{Z}\rvert)})$	(35) without multihop	6.11
△	Optimized	Equal	$\mathcal{O}(NFT_g(N^{\mathrm{Tx}}+2))$	CDS (Alg. 2)	6.95
□	Optimized	Equal	$\mathcal{O}(NFT_g(FT_g+(N^{\mathrm{Tx}})^2))$	[10]	5.88
+	Optimized	Equal	$\mathcal{O}(NN^{\mathrm{Tx}}FT_g)$	[68]	5.47

neighbors to communicate N^{Rx}. Note that the performance does not improve upon increasing N^{Rx} beyond 16, suggesting that a VUE typically can communicate only up to 16 closest neighbouring VUEs when $T = 12$. This implies that the number of receivers $N^{\mathrm{Rx}} = 20$ used for simulation results in Fig. 4–5 is sufficiently large.

To compare the fairness of the schemes, we plot the CDF for the connectivity of a VUE in Fig. 5 (a). The high slopes of the CDF show that the simple scheduling algorithms achieve better fairness compared to more advanced RRM schemes. Also, note that it is also possible to explicitly enforce fairness, as explained in Section III-C variant 3). Similarly, we plot the average connectivity of each VUE in a group of 20 VUEs (i.e., for $N^{\mathrm{Tx}} = 20$) in Fig. 5 (b). The VUE index $i \in \{0, 1, \cdots, 19\}$ on the horizontal axis corresponds to the position index of the VUE within the group. Note that for the algorithms supporting multihop, the connectivity is higher for VUEs in the middle of a group (see result for $8 \leq i \leq 11$), since these VUEs have more chances for multihoping within the group (we limit multihoping to be within a group for

simplicity of simulations). However, for the algorithms in [10] and [68], the performance is improved for edge users in the group. This can be due to the fact that edge VUEs can transmit more often to VUEs in the neighboring groups since those VUEs are not transmitting. On the other hand, VUEs within the group are transmitting themselves, hence have less chance for reception due to the half duplex criteria.

It is also worth mentioning that the performance loss due to clustering of the network is subject to G, N^{Tx}, T and multihop nature of the RRM schemes. If there are sufficient number of timeslots and multihop is not supported, then a VUE connectivity is saturated to approximately 6 neighbouring VUEs due to the noise limitations. Hence clustering will not affect the performance for no-multihop RRM schemes when there are sufficient number of timeslots. However, for multihop RRM schemes, the performance improves almost linearly with respect to T (see Fig. 4 (b)), however, increasing the size of the network worsen the connectivity marginally only (see Fig. 4 (a)). Since clustering effectively reduces the number of timeslots available for a VUE transmission, the performance loss can be significant. Our simulations show that splitting a network having 40 VUEs into two groups with each group having 20 VUEs, reduces the average VUE connectivity from 11.24 to 8.13, when $T = 12$. Hence a clustering approach is recommended mainly for the scalability of the network, i.e., to reduce the computational complexity or handle the case when the network controller is absent for the whole network.

VIII. Conclusions

This paper studies the multihop scheduling and power control performance of direct V2V multicast communication in the presence of CCI and ACI. From the study and results presented in this paper, we can draw the following conclusions,

1) The joint multihop scheduling and power control problem to maximize throughput/connectivity can be formulated as an MBLP problem. From this problem formulation, we can derive a scheduling-alone algorithm as a BLP problem and a power-control-alone algorithm as an MBLP problem. Similar problem formulation can be done to maximize worst-case throughput/connectivity as well.
2) To maximize connectivity with a required AoI/latency, the joint multihop scheduling and power control can be formulated as an MBLP problem.
3) The scalability issues of RRM schemes can be solved by splitting large networks into smaller clusters, and further splitting each cluster into smaller groups. Inter-group interference within a cluster can be avoided by allocating distinct timeslots to different groups and inter-cluster interference can be made to significantly low by appropriately choosing the cluster size. Each group can schedule and power control independently in its allocated timeslots, thereby, reducing the computational complexity.
4) In general the algorithms supporting multihop show significant performance improvement in maximizing the connectivity among vehicles.
5) The proposed CDS algorithm shows improved performance and works in a distributed manner without the need for channel knowledge.

Appendix A
A Mathematical Background

As already mentioned, we are trying to formulate all the problems into MBLP problems. However, we need to use nonlinear operations, like Boolean *OR*, *AND* and $\min$ operations. Therefore, in this appendix, we explain conversion of *OR*, *AND*, and $\min$ operations into linear constraints, and the whole paper assumes this conversion.

A. Converting OR operation into linear constraints

Let $x_1, x_2, \ldots x_n$ be Boolean variables. Let $y = x_1 \vee x_2 \vee x_3 \cdots \vee x_n$, be the *OR* value of all x values. In other words,

$$y = \bigvee_{i=1}^{n} x_i \tag{62}$$

We can translate the above nonlinear operation into the following linear constraints,

$$y \geq x_i \qquad \forall\, i \tag{63a}$$

$$y \leq \sum_{i=1}^{n} x_i \tag{63b}$$

$$y \in \{0, 1\} \tag{63c}$$

where (63c) ensures booleanity of y, the constraint (63b) ensures $y = 0$ when all x values are 0, and the constraint (63a) ensure $y = 1$ when any of the x values is 1. Therefore, the y variable satisfying all the constraints in (63) satisfies the equation (62).

B. Converting AND operation into linear constraints

Similarly *AND* operation (denoted by $\wedge$) can be translated into linear constraints. That is,

$$y = \bigwedge_{i=1}^{n} x_i \tag{64}$$

can be converted into the following linear constraints,

$$y \leq x_i \qquad \forall\, i \tag{65a}$$

$$y \geq \sum_{i=1}^{n} x_i - (n-1) \tag{65b}$$

$$y \in \{0, 1\} \tag{65c}$$

C. Converting min operation into linear constraints

In this section, we will show that the following problem can be translated into MBLP problem,

$$\min\ y \tag{66a}$$

s.t.

$$y = \min_i z_i \tag{66b}$$

That is, we want to minimize y but at the same time ensure that y is equal to the minimum of $\{z_1, z_2, \ldots, z_n\}$. This problem can be translated into

$$\min\ y \tag{67a}$$

s.t.

$$\sum_{i=1}^{n} \mathbb{1}\{y \geq z_i\} \geq 1 \tag{67b}$$

which can be further translated into the following MBLP,

$$\min\ y \tag{68a}$$

s.t.

$$y \geq z_i - \zeta(1 - w_i) \quad \forall i \tag{68b}$$

$$\sum_{i=1}^{n} w_i \geq 1 \tag{68c}$$

$$w_i \in \{0, 1\} \quad \forall i \tag{68d}$$

That is, we want to minimize y but at the same time ensure that y is greater or equal to at least one of the z_i values. The auxiliary Boolean variables w_i indicate if the constraint $y \geq z_i$ is satisfied or not, i.e., $w_i = \mathbb{1}(y \geq z_i)$. Observe that the constraint (67b) is equivalent to (68b)–(68d). The parameter ζ is a sufficiently large number to make constraint (68b) hold true when $w_i = 0$, for all possible values of z_i and y. It is not hard to prove that $\zeta = z^{\max} - z^{\min}$ is sufficient when the values of z are limited in an interval, i.e., $z_i \in [z^{\min}, z^{\max}], \quad \forall\, i$.

Note that the minimization in the AoI problem formulations discussed in Section III-C can be reduced to the above problem formulation (66), where constraint (24) can be thought as equivalent to (66b).

Appendix B
Some Practical Considerations

A. Supporting Large Message Payloads

If a message payload is too big to fit into an RB, then the message has to be fragmented into smaller packets and each packet has to be transmitted in separate RB. Assume that the message m is fragmented into a set of packets $\mathcal{P}_m$, and $X_{i,p,f,t} \in \{0, 1\}$ indicate if VUE i transmits the packet p in RB (f, t) or not. Then the constraint (21) is modified as follows,

$$W_{j,m,t} = \Big(\bigwedge_{p \in \mathcal{P}_m} \bigvee_{i=1}^{N} \bigvee_{f=1}^{F} (X_{i,p,f,t} \wedge Y_{i,j,f,t}) \Big) \wedge \Big(\bigwedge_{t'=0}^{t-1} \neg W_{j,m,t'} \Big) \tag{69}$$

B. Supporting Very Low Error Requirements

The standard approach to achieve low packet error probabilities is to use hybrid automatic repeat request (HARQ). However, this requires use of acknowledgements, which is cumbersome in broadcast communications and increases latency. For these reasons, we do not consider retransmission schemes in this paper. To achieve low error probabilities, we can use two other approaches: require higher SINR (which comes at the price of shorter 1-hop transmission range) or multiple repeated transmissions of the same message (which comes at the price of increased radio resource use). In the following, we will discuss both options.

For modern modulation and coding schemes, the packet error probability dependency on SINR can be divided into three SINR regions [70], [71]:

1) Low SINR region where the error probability close to 1
2) Medium SINR region where error probability decreases rapidly with SINR (also called the waterfall region)
3) High SINR region where error probability decreases relative slowly with SINR (also called the error-floor region)

Let $\epsilon(\gamma)$ denote the message error probability over one hop with SINR γ. Let us consider an end-to-end connection with h hops that are scheduled to respect the SINR threshold γ^{T}. That is, the hop SINRs $\gamma_1, \gamma_2, \ldots, \gamma_h$ are all greater or equal to γ^{T}. Since $\epsilon(\gamma)$ is nonincreasing with γ, $\epsilon(\gamma_\ell) \leq \epsilon(\gamma^{\mathrm{T}})$. Assuming hop errors are independent, the end-to-end error probability is

$$\epsilon^{\mathrm{e2e}}(\gamma_1, \gamma_2, \ldots, \gamma_h) = 1 - \prod_{\ell=1}^{h} (1 - \epsilon(\gamma_\ell)) \tag{70a}$$

$$\leq 1 - (1 - \epsilon(\gamma^{\mathrm{T}}))^h \tag{70b}$$

$$\leq 1 - (1 - \epsilon(\gamma^{\mathrm{T}}))^{N^{\mathrm{Tx}}} \tag{70c}$$

$$\leq N^{\mathrm{Tx}} \epsilon(\gamma^{\mathrm{T}}), \tag{70d}$$

where the inequalities follow since $\epsilon(\gamma_\ell) \leq \epsilon(\gamma^{\mathrm{T}})$, $h \leq N^{\mathrm{Tx}}$ (where N^{Tx} is the number of transmitters that is controlled by the scheduler), and $1 - (1 - x)^n \leq nx$ for $0 \leq x \leq 1,\ n \geq 1$.

Hence, for a given requirement ϵ^{req} on the end-to-end error probability for an arbitrary scheduled path through the network, we can guarantee that

$$\epsilon^{\mathrm{e2e}} \leq \epsilon^{\mathrm{req}}, \tag{71}$$

if we select γ^{T} such that

$$\gamma^{\mathrm{T}} = \min\{\gamma : \epsilon(\gamma) \leq \epsilon^{\mathrm{req}}/N^{\mathrm{Tx}}\}. \tag{72}$$

Note that this implies that we are using a higher SINR threshold than required when $h < N^{\mathrm{Tx}}$. However, if we operate in the waterfall region, the SINR penalty is small for modest N^{Tx}.

In the case increasing the SINR threshold is not attractive (perhaps because we are operating in the error-floor region), we can resort to using repeated transmissions. Suppose we fix γ^{T} such that the 1-hop error probability is upper bounded by $\epsilon(\gamma^{\mathrm{T}})$. The end-to-end error probability for scheduled

path with N^{Tx} hops is then $\epsilon^{\mathrm{e2e}} \leq N^{\mathrm{Tx}}\epsilon(\gamma^{\mathrm{T}})$. If errors occur independently, the error probability after ρ repeated transmissions over the end-to-end connection is $(\epsilon^{\mathrm{e2e}})^{\rho}$. To achieve the error probability ϵ^{req}, it is therefore enough to use $\rho = \lceil \log(\epsilon^{\mathrm{req}})/\log(N^{\mathrm{Tx}}\epsilon(\gamma^{\mathrm{T}}))\rceil$ repeated transmissions.

To support repeated transmissions, (21) has to be replaced by the following set of constraints,

$$\tilde{W}_{j,m,t} = \bigvee_{i=1}^{N}\bigvee_{f=1}^{F} X_{i,m,f,t} \wedge Y_{i,j,f,t} \tag{73a}$$

$$W_{j,m,t} \leq \rho + 1 - \sum_{t'=0}^{t} \tilde{W}_{j,m,t} + \zeta'(1 - W_{j,m,t}) \tag{73b}$$

$$W_{j,m,t} \geq \rho + 1 - \sum_{t'=0}^{t} \tilde{W}_{j,m,t} - \zeta'(1 - W_{j,m,t}) \tag{73c}$$

$$W_{j,m,t} \leq \bigwedge_{t'=0}^{t-1} \neg W_{j,m,t'} \tag{73d}$$

$$W_{j,m,t} \in \{0,1\} \tag{73e}$$

where $\tilde{W}_{j,m,t}$ indicate if message m is received by VUE j during timeslot t with 1-hop error probability ϵ. The constraints (73b) and (73c) are to ensure that $W_{j,m,t} = 0$, when $\sum_{t'=0}^{t} \tilde{W}_{j,m,t'} \neq \rho$. The parameter ζ' is a large number to make constraints hold when $W_{j,m,t} = 0$. It is not hard to prove that $\zeta' = T$ is sufficient. The constraint (73d) is to ensure that $W_{j,m,t} = 1$ only when the message is received for the first time with error probability less than or equals to ϵ^{req}. The main drawback with this scheme is that ρ repeated transmissions is used also when $h < N^{\mathrm{Tx}}$. This is wasteful, especially for 1-hop ($h = 1$) communication.

Appendix C
Age of Information Requirements

We recall from (24) that $A_{i,j,t}$ can be computed for $t \in \mathcal{S}$ as

$$A_{i,j,t} = \min_{m \in \mathcal{M}_i} (t + A_{i,j}^{\mathrm{init}} + 1 - (t_m^{\mathrm{gen}} + A_{i,j}^{\mathrm{init}} + 1) \sum_{t'=0}^{t} W_{j,m,t'}), \tag{74}$$

We see that $A_{i,j,t}$ is a deterministic function of t that depends on the scheduling and power allocation through $W_{j,m,t}$. Indeed, where we recall from (20) that

$$W_{j,m,t} = \begin{cases} 1, & \text{if message } m \text{ is } \textit{high-SINR scheduled} \\ & \text{to VUE } j \text{ for first time in timeslot } t \\ 0, & \text{otherwise} \end{cases} \tag{75}$$

That is, if $W_{j,m,t'} = 1$, then message m is scheduled to be transmitted by some VUE i' in an RB (f, t') where the received SINR at VUE j is high: $\gamma_{i',j,f,t'} \geq \gamma^{\mathrm{T}}$. Moreover, for all previous transmissions of message m, the received SINR at VUE j is less than γ^{T}.

However, the true AoI is a random process that depends on which messages that have been delivered error-free. We can find the true AoI, $A_{i,j,t}^{\mathrm{E}}$, by replacing $W_{j,m,t}$ in (74) with

$$W_{j,m,t}^{\mathrm{E}} = \begin{cases} 1, & \text{message } m \text{ is } \textit{delivered error-free} \text{ to} \\ & \text{VUE } j \text{ for first time in timeslot } t \\ 0, & \text{otherwise} \end{cases} \tag{76}$$

The superscript E is to indicate that the $W_{j,m,t}^{\mathrm{E}}$ and $A_{i,j,t}^{\mathrm{E}}$ are random due to transmission errors (which are random).

In general, $A_{i,j,t}$ is neither an upper nor a lower bound[4] on $A_{i,j,t}^{\mathrm{E}}$. Nevertheless, we will show that $A_{i,j,t}$ can be used to design a schedule and power allocation such that a probabilistic performance metric on $A_{i,j,t}^{\mathrm{E}}$ satisfies a predetermined requirement.

As mentioned in Section III-A7, we will consider probabilistic AoI requirements of the form

$$\Pr\{\mu(A_{i,j,t}^{\mathrm{E}}) \leq \mu^{\mathrm{T}}\} \geq P_A^{\mathrm{req}} \tag{77}$$

where the metric μ is a mapping from $(A_{i,j,t}^{\mathrm{E}} : t \in \mathcal{S})$ to $\mathbb{R}$, μ^{T} is the metric threshold, and P_A^{req} is the required probability. The metric μ is such that if $A'_{i,j,t} \leq A_{i,j,t}$ for $t \in \mathcal{S}$, then $\mu(A'_{i,j,t}) \leq \mu(A_{i,j,t})$.

Now suppose the schedule and power allocation is such that $\mu(A_{i,j,t}) \leq \mu^{\mathrm{T}}$. We will now show that this implies that $\Pr\{\mu(A_{i,j,t}^{\mathrm{E}}\} \leq \mu^{\mathrm{T}}\}$ is greater than a probability that can be controlled by the SINR threshold.

From (74), we see that $A_{i,j,t}$ is determined by $M_{i,j}$ scheduled transmissions, where

$$M_{i,j} = \sum_{m \in \mathcal{M}_i} \sum_{t=0}^{T-1} W_{j,m,t}. \tag{78}$$

That is, $M_{i,j}$ is the number of messages that are generated by VUE i and *high-SINR scheduled* to transmit to VUE j. We note that $M_{i,j} \leq |\mathcal{M}_i|$ since, for a fixed m and j, $\sum_{t=0}^{T-1} W_{j,m,t} \leq 1$. Let G denote the event that all of these *high-SINR scheduled* messages are delivered error-free. Assuming independent end-to-end message errors, we can write

$$\Pr\{G\} \geq (1 - \epsilon^{\mathrm{req}})^{M_{i,j}} \geq (1 - \epsilon^{\mathrm{req}})^{|\mathcal{M}_i|} \tag{79}$$

where the first inequality holds since γ^{T} is set sufficiently large to ensure that the end-to-end error probability $\epsilon^{\mathrm{e2e}} \leq \epsilon^{\mathrm{req}}$ (see Appendix B) and the second inequality holds since $M_{i,j} \leq |\mathcal{M}_i|$.

The crucial observation is that, conditioned on the event G, if $W_{j,m,t'} = 1$ for some message $m \in \mathcal{M}_i$, then message m is delivered error-free at timeslot t'. Hence, $W_{j,m,t''} = 1$ for some $t'' \leq t'$. The inequality is due to the facts that (a) conditioned on G, message m is delivered error-free at timeslot t' and (b) it is possible that the message m is transmitted in an

[4]To see this, suppose $W_{j,m,t'} = 1$. It is possible that the scheduled transmission at $t = t'$ suffers a transmission error, and message m is not delivered error-free at time slot t'. Moreover, it is also possible that the message m is delivered error-free in timeslot $t = t'' < t'$, although the SINR at t'' is less than γ^{T}.

RB (f'', t'') and delivered error-free, even though the SINR for this transmission is less than γ^{T}. (Fact (b) holds regardless if we condition on G or not). Now, additional received copies of message m cannot increase the AoI and it follows that, conditioned on G, $A^{\mathrm{E}}_{i,j,t} \leq A_{i,j,t}$ and

$$\mu(A^{\mathrm{E}}_{i,j,t}) \leq \mu(A_{i,j,t}) \leq \mu^{\mathrm{T}}. \tag{80}$$

Hence, if we by G^{c} denote the complement of the event G, we have that

$$\begin{aligned}
\Pr\{\mu(A^{\mathrm{E}}_{i,j,t}) \leq \mu^{\mathrm{T}}\} &= \Pr\{\mu(A^{\mathrm{E}}_{i,j,t}) \leq \mu^{\mathrm{T}} \mid G\} \Pr\{G\} \\
&\quad + \Pr\{\mu(A^{\mathrm{E}}_{i,j,t}) \leq \mu^{\mathrm{T}} \mid G^{\mathrm{c}}\} \Pr\{G^{\mathrm{c}}\} \\
&\geq \Pr\{\mu(A^{\mathrm{E}}_{i,j,t}) \leq \mu^{\mathrm{T}} \mid G\} \Pr\{G\} && \text{(81a)} \\
&= \Pr\{G\} && \text{(81b)} \\
&\geq (1 - \epsilon^{\mathrm{req}})^{|\mathcal{M}_i|}. && \text{(81c)}
\end{aligned}$$

where (81a) follows since probabilities are nonnegative, (81b) since $\Pr\{\mu(A^{\mathrm{E}}_{i,j,t}) \leq \mu^{\mathrm{T}} \mid G\} = 1$ due to (80), and (81c) follows from (79).

We can therefore conclude that the probabilistic requirement (77) is satisfied if $\mu(A_{i,j,t}) \leq \mu^{\mathrm{T}}$ and $(1 - \epsilon^{\mathrm{req}})^{|\mathcal{M}_i|} \geq P_A^{\mathrm{req}}$.

REFERENCES

[1] 3GPP, "5G; Service requirements for enhanced V2X scenarios," 3rd Generation Partnership Project (3GPP), TR, Oct. 2018. [Online]. Available: http://www.3gpp.org/ftp/Specs/html-info/22186.htm

[2] 3GPP, "Intelligent Transport Systems (ITS); Vehicular Communications; Basic Set of Applications; Part 3: Specifications of Decentralized Environmental Notification Basic Service," 3rd Generation Partnership Project (3GPP), TR 302.637, Apr. 2019. [Online]. Available: https://www.etsi.org/deliver/etsi_en/302600_302699/30263702/

[3] R. Devassy, G. Durisi, G. C. Ferrante, O. Simeone, and E. Uysal, "Reliable transmission of short packets through queues and noisy channels under latency and peak-age violation guarantees," *IEEE Journal on Selected Areas in Communications*, vol. 37, no. 4, pp. 721–734, Apr. 2019.

[4] S. Kaul, M. Gruteser, V. Rai, and J. Kenney, "Minimizing age of information in vehicular networks," in *2011 8th Annual IEEE Communications Society Conference on Sensor, Mesh and Ad Hoc Communications and Networks*, June 2011, pp. 350–358.

[5] A. Zaidi, F. Athley, J. Medbo, U. Gustavsson, G. Durisi, and X. Chen, *5G Physical Layer: Principles, Models and Technology Components*. Academic Press, May 2018.

[6] T. Abbas, F. Tufvesson, K. Sjöberg, and J. Karedal, "A measurement based shadow fading model for vehicle-to-vehicle network simulations," *International Journal of Antennas and Propagation*, May 2015.

[7] D. Vlastaras, T. Abbas, M. Nilsson, R. Whiton, M. Olbäck, and F. Tufvesson, "Impact of a truck as an obstacle on vehicle-to-vehicle communications in rural and highway scenarios," in *Proc. IEEE 6th International Symposium on Wireless Vehicular Communications*, Vancouver, Canada, Sept. 2014.

[8] R. Meireles, M. Boban, P. Steenkiste, O. Tonguz, and J. Barros, "Experimental study on the impact of vehicular obstructions in VANETs," in *2010 IEEE Vehicular Networking Conference*, Dec 2010, pp. 338–345.

[9] R. He, A. F. Molisch, F. Tufvesson, Z. Zhong, B. Ai, and T. Zhang, "Vehicle-to-vehicle propagation models with large vehicle obstructions," *IEEE Transactions on Intelligent Transportation Systems*, vol. 15, no. 5, pp. 2237–2248, Oct 2014.

[10] A. Hisham, E. G. Ström, F. Brännström, and L. Yan, "Scheduling and power control for V2V broadcast communications with co-channel and adjacent channel interference," *IEEE Access*, vol. 7, pp. 67 041–67 058, Jun. 2019.

[11] A. Hisham, D. Yuan, E. G. Ström, and F. Brännström, "Adjacent channel interference aware joint scheduling and power control for V2V broadcast communication," *to appear in IEEE Transactions on Intelligent Transportation Systems*, 2020.

[12] A. Mohammadi and F. M. Ghannouchi, *RF Transceiver Design for MIMO Wireless Communications*. Springer Berlin Heidelberg, 2012.

[13] P. M. Lavrador, T. R. Cunha, P. M. Cabral, and J. C. Pedro, "The linearity-efficiency compromise," *IEEE Microwave Magazine*, vol. 11, no. 5, pp. 44–58, Aug 2010.

[14] P. B. Kenington, "Linearized transmitters: an enabling technology for software defined radio," *IEEE Communications Magazine*, vol. 40, no. 2, pp. 156–162, Feb 2002.

[15] J. Chani-Cahuana, P. N. Landin, C. Fager, and T. Eriksson, "Iterative learning control for RF power amplifier linearization," *IEEE Transactions on Microwave Theory and Techniques*, vol. 64, no. 9, pp. 2778–2789, Sept 2016.

[16] G. Fodor, E. Dahlman, G. Mildh, S. Parkvall, N. Reider, G. Miklós, and Z. Turányi, "Design aspects of network assisted device-to-device communications," *IEEE Communications Magazine*, vol. 50, no. 3, pp. 170–177, Mar. 2012.

[17] N. Yu, J. Mei, L. Zhao, K. Zheng, and H. Zhao, "Radio resource allocation for D2D-based V2V communications with lyapunov optimization," in *2017 IEEE/CIC International Conference on Communications in China (ICC)*, Oct 2017.

[18] M. I. Ashraf, C. Liu, M. Bennis, W. Saad, and C. S. Hong, "Dynamic resource allocation for optimized latency and reliability in vehicular networks," *IEEE Access*, vol. 6, pp. 63 843–63 858, 2018.

[19] R. Molina-Masegosa, J. Gozalvez, and M. Sepulcre, "An IEEE 802.11p-assisted LTE-V scheduling for reliable multi-link V2X communications," in *2018 IEEE 88th Vehicular Technology Conference (VTC-Fall)*, Aug 2018.

[20] X. Zhang, Y. Shang, X. Li, and J. Fang, "Research on overlay D2D resource scheduling algorithms for V2V broadcast service," in *2016 IEEE 84th Vehicular Technology Conference (VTC-Fall)*, Sep. 2016.

[21] J. He, Z. Tang, Z. Fan, and J. Zhang, "Enhanced collision avoidance for distributed LTE vehicle to vehicle broadcast communications," *IEEE Communications Letters*, vol. 22, no. 3, pp. 630–633, March 2018.

[22] J. Lv, X. He, J. Li, H. Wang, and T. Luo, "Transmission capacity analysis of distributed scheduling in LTE-V2V mode 4 communication," in *Communications and Networking*, X. Liu, D. Cheng, and L. Jinfeng, Eds. Cham: Springer International Publishing, 2019, pp. 225–234.

[23] T. Sahin and M. Boban, "Radio resource allocation for reliable out-of-coverage V2V communications," in *2018 IEEE 87th Vehicular Technology Conference (VTC Spring)*, June 2018.

[24] J. Zhou, R. Q. Hu, and Y. Qian, "Message scheduling and delivery with vehicular communication network infrastructure," in *2013 IEEE Global Communications Conference (GLOBECOM)*, Atlanta, USA, Dec 2013, pp. 575–580.

[25] R. Fritzsche and A. Festag, "Location-based scheduling for cellular V2V systems in highway scenarios," in *2018 IEEE 87th Vehicular Technology Conference (VTC Spring)*, June 2018.

[26] C. Zhang, Y. Zang, J. A. L. Calvo, and R. Mathar, "A novel V2V assisted platooning system: Control scheme and MAC layer designs," in *2017 IEEE 28th Annual International Symposium on Personal, Indoor, and Mobile Radio Communications (PIMRC)*, Oct 2017.

[27] J. Tian and C. Lv, "Connectivity based transmit power control in VANET," in *2012 8th International Wireless Communications and Mobile Computing Conference (IWCMC)*, Aug 2012, pp. 505–509.

[28] H. Zhang, Y. Ma, D. Yuan, and H. Chen, "Quality-of-service driven power and sub-carrier allocation policy for vehicular communication networks," *IEEE Journal on Selected Areas in Communications*, vol. 29, no. 1, pp. 197–206, January 2011.

[29] F. Zeng, R. Zhang, X. Cheng, and L. Yang, "Channel prediction based scheduling for data dissemination in VANETs," *IEEE Communications Letters*, vol. 21, no. 6, pp. 1409–1412, 2017.

[30] Q. Wang, P. Fan, and K. B. Letaief, "On the joint V2I and V2V scheduling for cooperative VANETs with network coding," *IEEE Transactions on Vehicular Technology*, vol. 61, no. 1, pp. 62–73, Jan 2012.

[31] M. Jonsson, K. Kunert, and A. Böhm, "Increasing the probability of timely and correct message delivery in road side unit based vehicular communication," in *2012 15th International IEEE Conference on Intelligent Transportation Systems*, Sep. 2012, pp. 672–679.

[32] J. Wang, Y. Ji, X. Wang, and F. Liu, "RSU-coordinated multi-channel MAC with multi-criteria channel allocation," in *2012 International*

Conference on Connected Vehicles and Expo (ICCVE), Dec 2012, pp. 60–65.

[33] W. Li, X. Ma, J. Wu, K. S. Trivedi, X. L. Huang, and Q. Liu, "Analytical model and performance evaluation of long-term evolution for vehicle safety services," *IEEE Transactions on Vehicular Technology*, vol. 66, no. 3, pp. 1926–1939, March 2017.

[34] D. Li and Y. Liu, "In-band emission in LTE-A D2D: Impact and addressing schemes," in *2015 IEEE 81st Vehicular Technology Conference (VTC Spring)*, May 2015.

[35] H. Albasry, H. Zhu, and J. Wang, "The impact of in-band emission interference in D2D-enabled cellular networks," in *GLOBECOM 2017 - 2017 IEEE Global Communications Conference*, Dec 2017.

[36] L. Wang, X. Qi, and K. Wu, "Embracing adjacent channel interference in next generation WiFi networks," in *2016 IEEE International Conference on Communications (ICC)*, Kuala Lumpur, Malaysia, May 2016.

[37] A. Adya, P. Bahl, J. Padhye, A. Wolman, and L. Zhou, "A multi-radio unification protocol for IEEE 802.11 wireless networks," in *First International Conference on Broadband Networks*, San Jose, CA, USA, Oct 2004, pp. 344–354.

[38] J. Nachtigall, A. Zubow, and J. P. Redlich, "The impact of adjacent channel interference in multi-radio systems using IEEE 802.11," in *2008 International Wireless Communications and Mobile Computing Conference*, Crete Island, Greece, Aug 2008, pp. 874–881.

[39] C. Campolo, A. Molinaro, and A. Vinel, "Understanding adjacent channel interference in multi-channel VANETs," in *2014 IEEE Vehicular Networking Conference (VNC)*, Dec 2014, pp. 101–104.

[40] C. Campolo, C. Sommer, F. Dressler, and A. Molinaro, "On the impact of adjacent channel interference in multi-channel VANETs," in *2016 IEEE International Conference on Communications (ICC)*, May 2016.

[41] Y. Li, J. Luo, Z. Li, R. A. Stirling-Gallacher, W. Xu, and G. Caire, "Multihop routing in hybrid vehicle-to-vehicle and vehicle-to-infrastructure networks," in *2018 IEEE Globecom Workshops (GC Wkshps)*, Dec 2018.

[42] K. Dautov, S. Arzykulov, G. Nauryzbayev, and R. C. Kizilirmak, "On the performance of UAV-enabled multihop V2V FSO systems over generalized $\alpha - \mu$ channels," in *2018 International Conference on Computing and Network Communications (CoCoNet)*, Aug 2018, pp. 69–73.

[43] S. Tiwari and V. Bondre, "Performance evaluation of priority vehicle in multi-hop wireless network," in *2017 International Conference on Innovations in Information, Embedded and Communication Systems (ICIIECS)*, March 2017.

[44] G. Resta, P. Santi, and J. Simon, "Analysis of multi-hop emergency message propagation in vehicular ad hoc networks," in *Proceedings of the 8th ACM International Symposium on Mobile Ad Hoc Networking and Computing*, ser. MobiHoc. New York, USA: ACM, 2007, pp. 140–149. [Online]. Available: http://doi.acm.org/10.1145/1288107.1288127

[45] S. Ramanathan and E. L. Lloyd, "Scheduling algorithms for multihop radio networks," *IEEE/ACM Trans. Netw.*, vol. 1, no. 2, pp. 166–177, Apr. 1993. [Online]. Available: http://dx.doi.org/10.1109/90.222924

[46] A. Baiocchi and I. Turcanu, "A model for the optimization of beacon message age-of-information in a VANET," in *2017 29th International Teletraffic Congress (ITC 29)*, vol. 1, Sep. 2017, pp. 108–116.

[47] B. Zhou and W. Saad, "Joint Status Sampling and Updating for Minimizing Age of Information in the Internet of Things," *IEEE Transactions on Communications*, vol. 67, no. 11, pp. 7468–7482, Nov. 2019.

[48] M. A. Abd-Elmagid and H. S. Dhillon, "Average peak age-of-information minimization in UAV-assisted IoT networks," *IEEE Transactions on Vehicular Technology*, vol. 68, no. 2, pp. 2003–2008, Feb. 2019.

[49] W. Sun, E. G. Ström, F. Brännström, K. C. Sou, and Y. Sui, "Radio resource management for D2D-based V2V communication," *IEEE Transactions on Vehicular Technology*, vol. 65, no. 8, pp. 6636–6650, Aug 2016.

[50] E. Dahlman, S. Parkvall, and J. Sköld, *4G: LTE/LTE-Advanced for Mobile Broadband*. Oxford: Academic Press, 2011.

[51] R. T. Luttinen, "Statistical analysis of vehicle time headways," Ph.D. dissertation, Helsinki University of Technology, 1996. [Online]. Available: http://urn.fi/urn:nbn:fi:tkk-007970

[52] A. P. Florian and J. W. Stephen, "Interior-point methods," *Journal of Computational and Applied Mathematics*, vol. 124, no. 1, pp. 281–302, Dec. 2000.

[53] 3GPP, "Evolved Universal Terrestrial Radio Access (E-UTRA); Radio Frequency (RF) system scenarios," 3rd Generation Partnership Project (3GPP), TR 36.942, Oct. 2014. [Online]. Available: http://www.3gpp.org/ftp/Specs/html-info/36942.htm

[54] V. Vukadinovic, K. Bakowski, P. Marsch, I. Garcia, H. Xu, M. Sybis, P. Sroka, K. Wesolowski, DavidLister, and I. Thibault, "3GPP C-V2X and IEEE 802.11p for Vehicle-to-Vehicle communications in highway platooning scenarios," *Ad Hoc Networks*, vol. 74, 03 2018.

[55] E. Chan, "Overview of the sartre platooning project: Technology leadership brief," in *SAE Technical Paper*. SAE International, 10 2012. [Online]. Available: https://doi.org/10.4271/2012-01-9019

[56] Scania, "Annual report," Tech. Rep., 2001. [Online]. Available: http://www.scania.com/group/en/wp-content/uploads/sites/2/2015/09/sca01EN_tcm10-8527_tcm40-543841.pdf

[57] K. Koufos and C. P. Dettmann, "Temporal correlation of interference in vehicular networks with shifted-exponential time headways," *IEEE Wireless Communications Letters*, vol. 8, no. 1, pp. 189–192, Feb 2019.

[58] D. Kong and X. Guo, "Analysis of vehicle headway distribution on multi-lane freeway considering car-truck interaction," *Advances in Mechanical Engineering*, vol. 8, no. 4, 2016. [Online]. Available: https://doi.org/10.1177/1687814016646673

[59] R. J. Cowan, "Useful headway models," *Transportation Research*, vol. 9, no. 6, pp. 371 – 375, 1975. [Online]. Available: http://www.sciencedirect.com/science/article/pii/0041164775900088

[60] 3GPP, "Technical specification group radio access network; study on LTE-based V2X services," 3rd Generation Partnership Project (3GPP), TR 36.885, June 2016. [Online]. Available: http://www.3gpp.org/ftp/Specs/html-info/36885.htm

[61] ——, "Intelligent Transport Systems (ITS); LTE-V2X Access layer specification for Intelligent Transport Systems operating in the 5 GHz frequency band," 3rd Generation Partnership Project (3GPP), TR 303.613, May 2019. [Online]. Available: https://www.etsi.org/deliver/etsi_en/302600_302699/30263702/

[62] ——, "LTE; Evolved Universal Terrestrial Radio Access (E-UTRA); Physical layer procedures," 3rd Generation Partnership Project (3GPP), TR 36.213, March 2019. [Online]. Available: http://www.3gpp.org/ftp/Specs/archive/36_series/36.213/

[63] J. Karedal, N. Czink, A. Paier, F. Tufvesson, and A. Molisch, "Path loss modeling for vehicle-to-vehicle communications," *IEEE Transactions on Vehicular Technology*, vol. 60, no. 1, pp. 323–328, Jan. 2011.

[64] T. Abbas, J. Nuckelt, T. Kürner, T. Zemen, C. F. Mecklenbräuker, and F. Tufvesson, "Simulation and measurement-based vehicle-to-vehicle channel characterization: Accuracy and constraint analysis," *IEEE Transactions on Antennas and Propagation*, vol. 63, no. 7, pp. 3208–3218, July 2015.

[65] L. Cheng, B. E. Henty, F. Bai, and D. D. Stancil, "Highway and rural propagation channel modeling for vehicle-to-vehicle communications at 5.9 GHz," in *2008 IEEE Antennas and Propagation Society International Symposium*, July 2008.

[66] J. Kunisch and J. Pamp, "Wideband car-to-car radio channel measurements and model at 5.9 GHz," in *Proceedings IEEE Vehicular Technology Conference*, Sept 2008.

[67] M. G. Nilsson, C. Gustafson, T. Abbas, and F. Tufvesson, "A measurement-based multilink shadowing model for V2V network simulations of highway scenarios," *IEEE Transactions on Vehicular Technology*, vol. 66, no. 10, pp. 8632–8643, Oct 2017.

[68] B. Peng, C. Hu, T. Peng, Y. Yang, and W. Wang, "A resource allocation scheme for D2D multicast with QoS protection in OFDMA-based systems," in *2013 IEEE 24th Annual International Symposium on Personal, Indoor, and Mobile Radio Communications (PIMRC)*, Sept 2013, pp. 2383–2387.

[69] Gurobi Optimization, Inc., "Gurobi optimizer reference manual," 2015. [Online]. Available: http://www.gurobi.com

[70] W. Ryan and S. Lin, *Channel Codes: Classical and Modern*. Cambridge University Press, 2009.

[71] T. Richardson, "Error-floors of LDPC codes," in *Proceedings of the 41st Annual Conference on Communication, Control and Computing*, 2003, pp. 1426–1435.

Anver Hisham received the M. Tech. degree in communication systems from Indian Institute of Technology, Madras, India in 2010. From 2010 to 2014, he was a research engineer in Centre of Excellence in Wireless Technology, Chennai, India. He received his PhD degree with Communication Systems Group in Chalmers University of Technology, Gothenburg, Sweden, in 2019. Currently he is working in Combitech AB, Sweden, as research engineer. His research focuses mainly upon physical and MAC layer of 5G systems. He is also interested in wireless communication simulations, modeling and optimization.

Erik G. Ström (S'93–M'95–SM'01) received the M.S. degree from the Royal Institute of Technology (KTH), Stockholm, Sweden, in 1990, and the Ph.D. degree from the University of Florida, Gainesville, in 1994, both in electrical engineering. He accepted a postdoctoral position at the Department of Signals, Sensors, and Systems at KTH in 1995. In February 1996, he was appointed Assistant Professor at KTH, and in June 1996 he joined Chalmers University of Technology, Göteborg, Sweden, where he is now a Professor in Communication Systems since June 2003. Dr. Ström currently heads the Division for Communication and Antenna Systems, is the director of ChaseOn, a Vinnova Competence Center focused on antenna system, and leads the competence area Sensors and Communications at the traffic safety center SAFER, which is hosted by Chalmers. His research interests include signal processing and communication theory in general, and constellation labelings, channel estimation, synchronization, multiple access, medium access, multiuser detection, wireless positioning, and vehicular communications in particular. Since 1990, he has acted as a consultant for the Educational Group for Individual Development, Stockholm, Sweden. He is a contributing author and associate editor for Roy. Admiralty Publishers FesGas-series, and was a co-guest editor for the *Proceedings of the IEEE* special issue on Vehicular Communications (2011) and the *IEEE Journal on Selected Areas in Communications* special issues on Signal Synchronization in Digital Transmission Systems (2001) and on Multiuser Detection for Advanced Communication Systems and Networks (2008). Dr. Ström was a member of the board of the IEEE VT/COM Swedish Chapter 2000–2006. He received the Chalmers Pedagogical Prize in 1998 and the Chalmers Ph.D. Supervisor of the Year award in 2009.

Fredrik Brännström (S'98–M'05) received the M.Sc. degree from Luleå University of Technology, Luleå, Sweden, in 1998, and the Ph.D. degree in Communication Theory from the Department of Computer Engineering, Chalmers University of Technology, Gothenburg, Sweden, in 2004. From 2004 to 2006, he was a Post-Doctoral Researcher at the Department of Signals and Systems, Chalmers University of Technology. From 2006 to 2010, he was a Principal Design Engineer with Quantenna Communications, Inc., Fremont, CA, USA. He is currently Professor and Head of Communication Systems Group, Department of Electrical Engineering, Chalmers University of Technology, Gothenburg, Sweden. He was a recipient of the 2013 IEEE Communication Theory Workshop Best Poster Award. In 2014, he received the Department of Signals and Systems Best Teacher Award. He has co-authored the papers that received the 2016 and 2017 Best Student Conference Paper and the 2018 Best Student Journal Paper, all awarded by the IEEE Sweden Joint VT-COM-IT Chapter. His current research interests include algorithms, resource allocation, synchronization, antenna concepts, and protocol design for vehicular communication systems, as well as different applications of coding.